Protein Kinase C Substrates That Drive Motility of Cancer Cells

By

Xiangyu Chen

A dissertation submitted to the Graduate Faculty in Biochemistry

in partial fulfillment of the requirements for the degree of

Doctor of Philosophy

The City University of New York

2010

This manuscript has been read and accepted for the Graduate Faculty in Biochemistry in satisfaction of the dissertation requirement for the degree of Doctor of Philosophy.

Dr. Susan A. Rotenberg

_____	_____
Date	Chair of Examining Committee

Dr. Edward J. Kennelly

_____	_____
Date	Executive Officer

Dr. Wilma Saffran

Dr. Karl Fath

Dr. Jill Bargonetti

Dr. Jeffrey Segall
Supervisory Committee

THE CITY UNIVERSITY OF NEW YORK

ABSTRACT

Protein Kinase C Substrates That Drive Motility of Cancer Cells

By
Xiangyu Chen

Advisor: Dr. Susan A Rotenberg

As the intracellular receptor of tumor promoting phorbol esters, protein kinase C (PKC) is functionally linked to carcinogenesis and metastasis. Therefore, it is crucial to identify substrates of PKC in order to understand the mechanisms by which these substrate proteins participate in cancer-related phenotypes such as motile behavior. The work to be described consists of two projects: 1) new PKC substrates that contribute to the motility phenotype of human breast cells, and 2) the role of a known PKC substrate, MARCKS (Myristoylated Alanine-Rich C-Kinase Substrate) in the motility pathway of mouse melanoma cells.

To identify direct substrates, a chemical-genetic approach was used to engineer the ATP binding site of PKC-α, δ and ζ to enable them to bind an unnatural ATP analogue. Consequently, phosphorylation is attributed exclusively to the mutant enzyme, and the phosphorylated protein bands are potential substrates. Following expression in human breast cells (MCF-10A), co-immunoprecipitation of the mutant enzyme bound with high affinity protein substrates was carried out. Following addition of an ATP analogue, a number of phosphorylated proteins were produced and subsequently analyzed by mass spectrometry. PKC-α and δ traceable kinases had very similar phosphorylation patterns, whereas the profile for PKC-ζ was distinct. Several potential protein substrates involved in cytoskeletal structure were identified for PKC-α and PKC-δ, including proteins that bind small GTP-binding proteins (Rho Kinase-1, Cdc42ep4, Rho/cdc42/Rac activating protein-1), as well as proteins

that had been previously documented as PKC substrates (IQGAP, VASP).

In a second project, the role of MARCKS was investigated in the context of mouse melanoma cell motility. As a protein that is known to crosslink actin bundles to the plasma membrane, this PKC substrate has been linked with cell migration and adhesion. Upon phosphorylation by PKC, MARCKS is released into the cytoplasm, thereby promoting actin rearrangement. Weakly metastatic B16 F1 cells do not express detectable phospho-MARCKS. However, F1 cells that are engineered to express a pseudo-phosphorylated mutant of MARCKS exhibit elevated motility. When F1 cells are treated with okadaic acid (OA), an inhibitor of protein phosphatases, increases in both phospho-MARCKS and motility are observed. OA-induced motility can be substantially eliminated when cells are pre-treated with a shRNA reagent to knock down MARCKS expression, or when expressing a phosphorylation-resistant mutant of MARCKS. Furthermore, a phosphorylation-resistant MARCKS mutant that was made exclusively cytoplasmic due to lack of a myristoyl group was observed to inhibit motility of OA-treated F1 cells as well as motility of highly metastatic melanoma cells (mouse F10 and human A375 cells). These findings imply that MARCKS promotes motility through cytoplasmic interactions involving its phosphorylated effector domain. It is concluded that phospho-MARCKS has a previously undocumented role in the cytoplasm that promotes motile behavior and possibly the metastatic potential of many different cancer cells.

Overall, this work describes substrates of PKC that transmit the motility signal in cancer cells, and suggests novel targets for the development of anti-metastasis agents.

ACKNOWLEDGEMENTS

I would like to thank my mentor, Dr. Susan A Rotenberg. I could have never achieved my degree without her guidance. Thanks to my examining committee, Dr. Wilma Saffran, Dr. Karl Fath, Dr. Jill Bargonetti, and Dr. Jeffrey Segall for their insightful comments during each meeting and time spent reading my thesis. I would also like to thank the faculty and staff in the Department of Chemistry and Biochemistry at Queens College, the City University of New York.

Thank you to Dr. Areti Tsiola for her assistance in operating the confocal and fluorescence microscopes and for reading my thesis draft.

My special thanks to former Rotenberg lab members, Dr. Thushara Abeyweera and Dr. Regina Sullivan for their technical assistance and enlightening discussions.

Finally, I am always grateful to my parents and my wife for their financial and spiritual support. Their understanding and encouragement helped me through my hard but also fulfilling journey to my Ph.D. degree.

Dedication

This thesis is dedicated to my mentor, Dr. Susan A Rotenberg.

TABLE OF CONTENTS

List of Tables **Page**

List of Figures **Page**

Abbreviations Used

ATP	adenosine triposphate
A*TP	N^6-phenyl-ATP
BSA	bovine serum albumin
DAG	diacylglycerol
DTT	dithiothreitol
EDTA	N, N, N', N'-ethylenediaminetetraacetic acid
EGF	epidermal growth factor
EGTA	ethylene glycol-*bis* (2-aminoethylether)-N,N,N',N'-tetraacetic acid
FBS	fetal bovine serum
GFP	green fluorescent protein
MAPK	mitogen activated protein kinase
MARCKS	myristoylated alanine-rich C kinase substrate
MBP	myelin basic protein
MS	mass spectrometry
OA	okadaic acid
PCR	polymerase chain reaction
PDK-1	phosphoinositide-dependent kinase-1
PICK	protein that interacts with C-kinase
PKA	cAMP-dependent protein kinase
PKC	protein kinase C
PS	phosphatidylserine
RACK	receptor for activated C kinase
RIPA	radioimmune precipitation assay
RFP	red fluorescent protein
RT-PCR	real time polymerase chain reaction
shRNA	small hairpin ribonucleic acid
TPA	12-***O***-tetradecanoylphorbol-13-acetate

CHAPTER 1

INTRODUCTION

Protein kinase C (PKC) is a multi-functional serine/threonine protein kinase. The first PKC members were identified in bovine brain by Nishizuka and co-workers in 1977 (Nishizuka, 1984; Ekker and Parker, 1994). PKC comprises a super-family of 11 structurally-related isoforms that have distinct and overlapping cellular functions. These isoforms serve key regulatory roles in cell proliferation, apoptosis, migration, adhesion, cytoskeletal dynamics, and metastasis.

PKC Activation and Classification

As shown in Figure 1, PKC activation in mammalian cells requires the presence of diacylglycerol (DAG) and calcium ions (Ca^{2+}). Growth factors (such as EGF) trigger increased levels of these PKC activators by stimulating receptors that are coupled to membrane-associated phospholipase C (PLC). This enzyme cleaves phosphatidylinositol 4,5 *bis*-phosphate (PIP_2) resulting in the formation of DAG plus inositol-1,4,5-triphosphate (IP_3). Consequently, IP_3 elicits the release of Ca^{2+} from the endoplasmic reticulum (ER) lumen. Upon binding to elevated levels of DAG and Ca^{2+}, cytoplasmic PKC is recruited to the plasma membrane by a process called “translocation”. While associated with the membrane, PKC phosphorylates protein substrates that participate in a variety of cellular responses. However, only a few proteins have been identified as PKC substrates having functional significance.

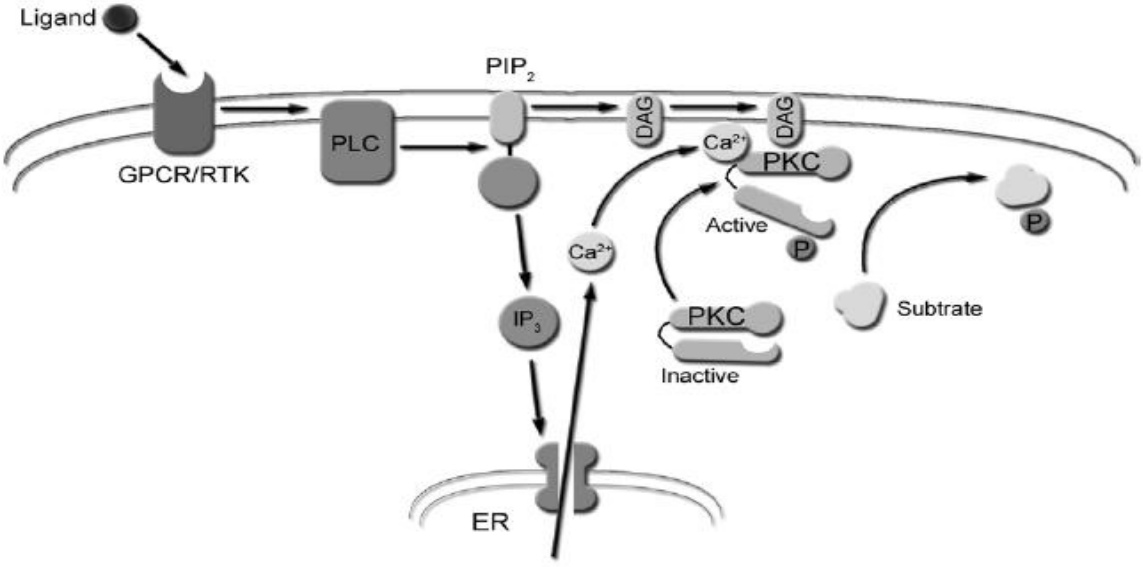

Figure 1. Activation of conventional PKC by an extracellular signal via G-coupled receptors. (Koivunen *et al*, 2005)

The eleven known PKC isoforms are sub-divided into three sub-categories according to the means by which they are activated. Conventional PKC isoforms (α, βI, βII and γ) require DAG and Ca^{2+}, while novel PKCs (δ, ε, η, θ) require only DAG. Atypical PKCs, namely ζ and ι, are not regulated by either DAG or Ca^{2+}, but can be activated by lipids such as IP_3 and ceramide (Bourbon *et al*., 2000). In view of their differing regulation, PKC isoforms carry out distinct and overlapping responses to extracellular stimuli. These responses are apparently dependent on the cell type in which the isoforms are expressed, where a given cell type has a characteristic isoform expression profile. PKCα is a universally expressed isoform and has been linked variously to cell growth, proliferation, adhesion and migration depending on the cell type under study (Ghoul *et al*., 2006).

PKC Structure

PKC isoforms have a single polypeptide chain with an N-terminal regulatory domain and a C-terminal catalytic domain connected by a hinge region (Figure 2).

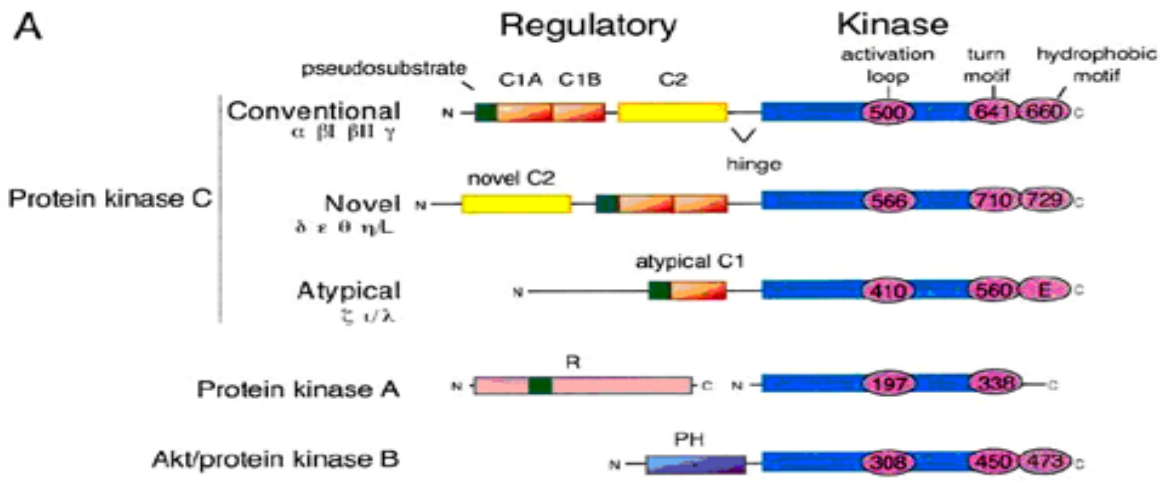

Figure 2. Domain composition of ABC protein kinase family members (Newton, 2003)

The cysteine-rich C1 domain contains the binding site for diacylglycerol, the same site recognized by the phorbol ester TPA (tetradecanoyl-12-phorbol-13-acetate), a potent PKC activator and tumor promoter produced in plants. Binding to the C1 domain by DAG or TPA creates a continuous hydrophobic surface on the enzyme that greatly enhances its membrane interactions. The C2 domain has a globular structure and contains the Ca^{2+} binding site. Conventional PKCs have functional C1 and C2 domains enabling them to be activated by both diacylglycerol and Ca^{2+}, whereas novel (Ca^{2+}-independent) PKCs lack a functional C2 domain but contain a functional C1 domain that makes them responsive to DAG. Because atypical PKCs do not contain a C2 domain and only a partial C1 domain, they cannot be activated by diacylglycerol or Ca^{2+}. However, the atypical isoforms can be activated by other lipids such as ceramide (Bourbon *et al.*, 2000). Endogenous PKCs are maintained in an inactive

conformation due to the binding of the pseudosubstrate sequence (located in the amino terminal region) to the substrate binding site in the catalytic domain (see Figure 2). Upon activation of PKC by DAG and Ca^{2+}, the pseudosubstrate is released from the substrate binding pocket, thereby allowing exogenous protein substrates to bind and undergo phosphorylation. When activated, PKC is re-distributed to various intracellular locations to perform phosphorylation of substrates. The sub-cellular distribution of PKC isoforms is determined by anchoring proteins that serve as an extremely important control of this pivotal kinase (Sukai and Mochly-Rosen, 1999). Following their activation, PKC isoforms can undergo down-regulation due to the actions of calpain, resulting in the termination of the signal (Murray *et al*., 1987; Kikkawa *et al*., 1989).

The conformation of the catalytic domain contains binding sites for ATP and protein substrates. This conformation is well conserved in the ABC kinase family. Following protein synthesis, PKC undergoes maturation by a series of phosphorylation events in the catalytic domain: an initiating transphosphorylation by phosphoinositide-dependent kinase-1 (PDK-1) at the activation loop, followed by autophosphorylation events at the turn motif and hydrophobic motif. As shown in Figure 3, the three phosphorylation sites are highly conserved among all 11 isoforms of PKC, as well as in other related protein kinases.

PKC and Cancer

The potent binding and activation of PKC by the tumor promoter TPA was the first indication that PKC activity is linked to cancer progression (Castagna *et al*., 1982). Upon activation by

nanomolar concentrations of TPA, PKC stimulates diverse cell responses that affect the rate of proliferation, morphology, movement and survival (Dempsey *et al*., 2000). Of the three subfamilies, PKC-α, δ and ζ are the most widely expressed in all tissue types, while others are tissue specific (Mellor and Parker, 1998; Nishizuka, 1989). In many cancer cell lines, such as melanoma cells, PKCα is the most abundantly expressed isoform.

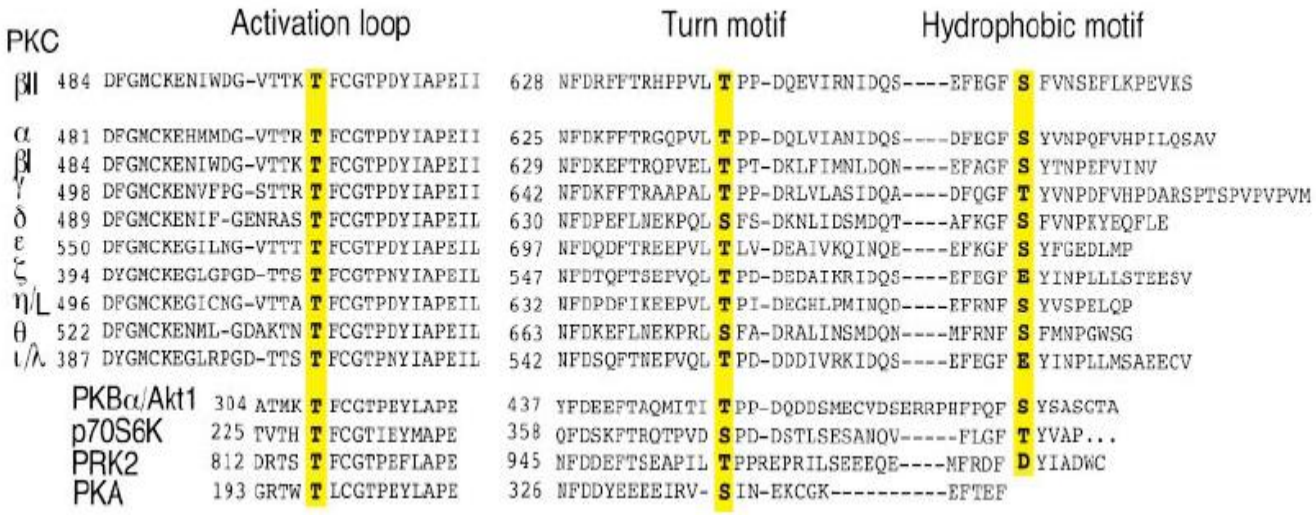

Figure 3. Alignment of activation loop, turn motif and hydrophobic motif of PKC isoforms, Akt and PKA. (Newton, 2003).

In various cancers, including melanoma and breast tumors, the α-isoform of PKC has been associated with tumor progression and metastasis. Previous studies showed that over-expression of wildtype PKCα in non-transformed non-motile human breast MCF-10A cells causes a dramatic increase in cell motility (Sun and Rotenberg, 1999). Similarly, when B16 F1 mouse melanoma cells are treated with TPA, they gain metastatic potential that is comparable with B16 F10 cells, a sub-line with highly invasive behavior (Gopalakrishna and Barsky, 1988). In some studies it has been shown that many high-grade invasive tumors express elevated levels of PKCα (Wetsel *et al*., 1992). This evidence shows a direct linkage

between PKCα expression and cell invasiveness that is the hallmark of metastasis. However in advanced breast tumors, PKCα is often down-regulated (Kerfoot *et al*., 2004), thereby suggesting that other PKC isoforms such as PKC-δ, may promote metastasis (see below). As cell movement is an aspect of cancer metastasis, it is not surprising that many intracellular PKCα substrates are associated with the cytoskeleton. Most evidence gathered to date is consistent with PKCα serving a role in the metastatic phenotype.

Similarly, PKCδ expression levels were observed to be very high in breast cancers, as shown by Real-Time PCR. These increased expression levels correlated with a poor prognosis (McKiernan *et al*., 2008), thereby indicating a stimulating role of PKCδ during cancer progression. Furthermore, the ability of PKCδ to activate MAP kinase often correlates with an oncogenic outcome (Ueda *et al*., 1996). The primary evidence that ties PKCδ to cell migration comes from studies in which cytoskeletal proteins such as integrins, myosin light chain and adducins were shown to have been phosphorylated by PKCδ (Alt *et al*., 2004; Iwabu A *et al*., 2004; Kiley *et al*., 1999). In a separate study, PKCδ phosphorylated α6β4 integrin dimers and caused disassembly of hemidesmosomes. The subsequent loss of stable adhesion in turn facilitated basal cell migration (Alt *et al*., 2004). When weakly metastatic cells were engineered to stably express wildtype PKCδ, they acquired increased anchorage-independent growth, which often accompanies metastasis as a result of decreased attachment to the matrix (Kiley *et al*., 1999). PKCδ was also found to be elevated at both the mRNA level and the protein level in highly invasive rat mammary tumor cells when compared to cells with low metastatic potential. Taken together, these findings suggest that in breast cells, PKCδ has a

pro-metastatic effect.

The atypical form PKCζ is another important PKC member which regulates cell functions such as proliferation and migration. Although its role in growth regulation is apparently cell-type dependent, PKCζ suppresses Ras-induced lung carcinogenesis in mice by inhibiting interleukin-6 production, consequently promoting tumor cell growth under nutrient-deprived conditions (Galvez *et al*., 2009). Consistent with its apparent anti-carcinogenic effect, PKCζ was shown to inhibit migration of B16 F1 mouse melanoma cells through an interaction with PAR-4 (Sanz-Navarez *et al*., 2001). This finding suggests that PKCζ has an anti-metastatic role. Moreover, in normal mouse mammary cells stably transfected with wildtype PKCζ, adhesion was enhanced and cell migration was greatly inhibited when examined by wound healing assay (Urtreger *et al*., 2005). Thus, by controlling key steps such as adhesion and migration in metastasis, PKCζ exerts a suppressive role in cancer metastasis that contrasts with the functions of PKC-α and δ.

Tumor metastasis

Metastasis is the process by which a cell of the primary tumor dissociates and is disseminated throughout the body. For a tumor cell to metastasize, the cell must be able to move out of the original tumor and enter the circulation (intravasation) in a process that involves the release of proteases such as urinary-type plasminogen activator. The blood borne tumor cell exits the circulation by first adhering to capillary walls (extravasation) and invades other tissues such as lung (Figure 4).

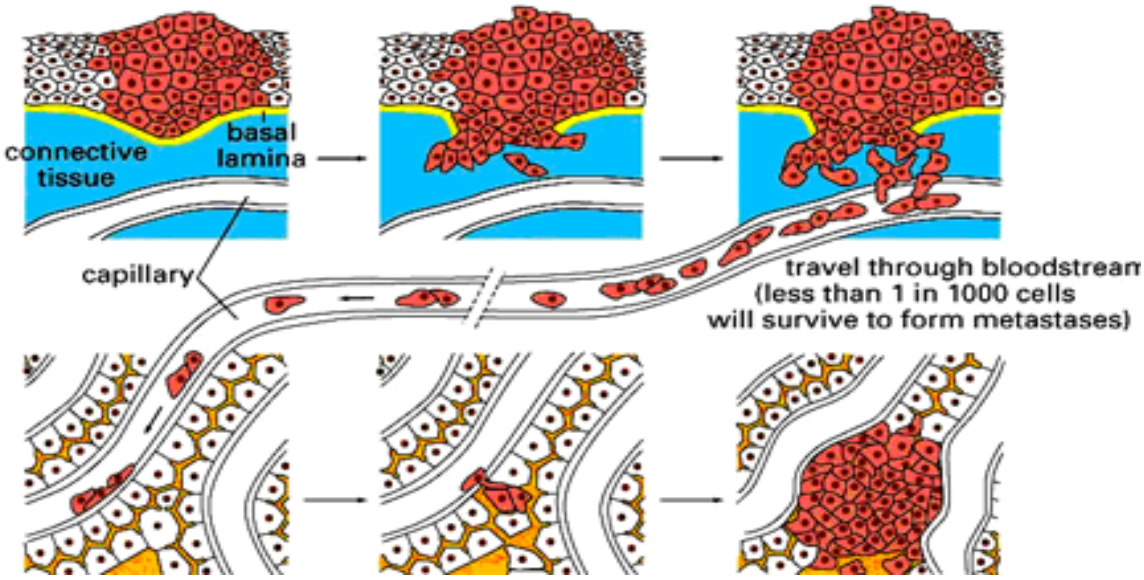

Figure 4. Events that define the process of metastasis (Alberts *et al*., 2002)

Because PKC promotes adhesion and cell movement of cancer cells (breast, melanoma, etc.), its catalytic activity is somehow involved in the metastatic process. The Rotenberg lab demonstrated that, in murine melanoma cells, motility is inhibited upon expression of dominant negative (kinase-dead) PKCα (Sullivan *et al*., 2000). Because of the availability of a mouse model (C57BL/6) that is syngeneic with B16 murine melanoma cells, the B16 cell line offers an excellent model to examine the effect of PKCα activity on cell behavior *in vitro* and to correlate the results with comparable *in vivo* studies. Two related B16 sub-lines with differing metastatic potential are F1 cells, which are weakly metastatic, and F10 cells, which are highly metastatic in C57BL/6 mice (Gopalakrishna and Barsky, 1988). Following *in vitro* manipulation of PKC activity in either cell line - by transfection with either mutant PKCα cDNA or treatment with inhibitors - the metastatic potential can be measured by injecting cells into the tail vein of the C57BL/6 mouse, and subsequently counting the nodules that form in the lung following pulmonary colonization. Various PKC isoforms are expressed in B16

melanoma cells where PKCα is the most abundant (Becker *et al.*, 1990). Although it has been shown that PKCα and PKCβ both increase melanin synthesis in murine melanoma cells (Gordon and Gilchrest, 1989), the precise substrate remains unknown. However, linkage between melanogenesis and cell migration has not been demonstrated, suggesting that the two phenotypes occur by distinct pathways via different PKC substrates (Sanz-Navares *et al*., 2001).

PKC in cell adhesion and motility

Cell movement arises from a series of events consisting of protrusion, adhesion and retraction steps. To initiate movement, the cell protrudes the plasma membrane (via lamellapodia or filopodia) that establishes adhesion to the extracellular matrix. Interaction between the cell membrane and the matrix requires membrane-associated integrin proteins that bind the matrix and provide adhesive strength. Many proteins, including focal adhesion kinase (FAK), are recruited to the focal adhesion site when the cell is making contact with the matrix. It has been shown that in MCF-7 human breast cells that had been engineered to overproduce PKCα (Ng *et al*., 1999), PKCα interacts with β1 integrin to promote movement of integrin to the tip of the filopodia. Upon treatment of MCF-7 transfectants with TPA, the cells were found to have increased migration on fibronectin, laminin, or collagen substrates, and implied a role of PKCα in regulating adhesion. Similarly, when B16 F10 cells were engineered to over-express a kinase-defective form of PKCα, they exhibited a substantial decrease in migration and adhesion to collagen IV, as shown in Figure 5 (Sullivan *et al*., 2000).

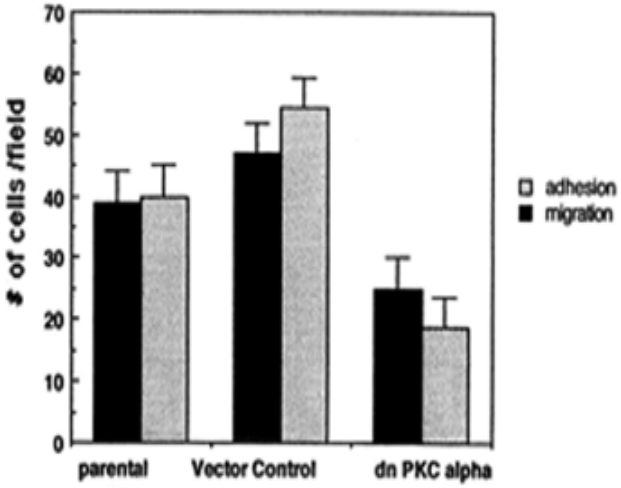

Figure 5. Inhibition of adhesion and migration on collagen IV of B16 F10 cells transfected with kinase-defective PKCα. To assay migration, 12-well Costar polycarbonate Boyden chambers were coated with 2μg/cm^2 collagen IV. Cells were seeded at 10^5 cells per well and incubated for 3 h at 37 °C, 5% CO_2. Cells that migrated across the microporous filter were stained and counted. Results are representative of three independent experiments. Error bars, +/- S.D. $p < 0.001$. [Dark bars, migration; gray bars, adhesion]. (Sullivan *et al.*, 2000)

PKC substrates

Until recently, elucidation of PKC-mediated pathways was made difficult by the absence of a suitable technique to identify direct substrates of a protein kinase. This challenge arises from the fact that once a phospho-protein is formed, it is almost impossible to identify the protein kinase that produced it. The presence of a phosphorylation site known to be recognized by a specific protein kinase (its consensus sequence) is helpful, but can be complicated by the possibility that more than one protein kinase will recognize this site due to overlapping substrate specificities.

Although PKC is known to phosphorylate many substrates *in vitro*, only a limited number of proteins have been identified as intracellular substrates whose phosphorylation has functional significance for the cell. The two major biochemical approaches that were traditionally

employed to identify intracellular PKC substrates have exploited those attributes that distinguish PKC from other protein kinases. The first approach was to pre-label the intracellular ATP pool by treating cells with radioactive phosphate (^{32}P), followed by treatment with TPA to produce a pattern of radiolabeling that was due to PKC activation. Because TPA activates several isoforms (conventional and novel isoforms), this method was not isoform-specific. Furthermore, the radiolabeling pattern would also potentially include ^{32}P-labeled protein substrates of protein kinases lying downstream in a pathway activated by PKC. In a different approach, the known consensus sequence of PKC (Kennelly and Krebs, 1991), namely $K/R_{1-3}X_{0-2}S/TX_{0-2}R/K_{1-3,}$ can be used to search primary protein sequences for PKC-related recognition sequence motifs, followed by a determination of whether this protein undergoes radiolabeling in cells treated with TPA. With the availability of isoform-specific antibodies, a third approach could use immunoprecipiation of a PKC isoform as a means to identify binding partners that may serve also as substrate proteins.

Given below is a listing of proteins that have been characterized as intracellular PKC substrates.

Adducin was first identified in 1986 in the red blood cell membrane (Gardner and Bennett, 1986) and was found to undergo rapid phosphorylation upon TPA treatment (Ling *et al*., 1986). It is a protein that caps and assembles actin filaments with spectrin, a cytoskeletal protein in erythrocyte membranes. This process is critical for maintaining the shape of red blood cells. Once phosphorylated by PKC, the ability of adducin to cap actin filaments is decreased.

Fascin bundles actin filaments and is important in cell movement, especially in the protrusion step. It was identified in 1978 as an actin-interacting protein from sea urchin (Brian and Kane, 1978). By aligning the cDNA sequence across different species, a consensus motif for phosphorylation by PKC was located between amino acid residues 11 and 50 (Kureishy *et al*., 2002). Like adducin, phosphorylation of fascin by PKC on a serine residue inhibits its activity.

ERM (ezrin-radixin-moesin) proteins function as connectors of the microfilaments with the plasma membrane. They also play a role in signal transductions. Phosphorylation of these proteins by different PKC isoforms inhibits their activity. For example, moesin was found to be phosphorylated by PKCθ (Pietromonaco *et al*., 1998).

AFAP-110 is a multi-domain protein that is believed to transduce PKC signals to the cytoskeleton. It can cross-link actin filaments and bind to Src kinase through SH2 and SH3 domains and thereby activate it. By analysis of its primary sequence, AFAP-110 was predicted to be a PKC substrate (Flynn *et al*., 1993). This prediction was later confirmed experimentally (Qian *et al*., 2002). Once phosphorylated by classical PKCs, AFAP-110 is able to activate Src kinase.

Vinculin has been shown to undergo increased phosphorylation in cells by treatment with Ca^{2+} and TPA (Werth and Pastan, 1983), and was confirmed to serve as a direct PKC substrate *in vitro*. Vinculin functions as an intracellular anchoring protein that connects actin filaments and integrins in cell-cell junctions and the cell-matrix adhesion process.

β4-Integrin is a key protein involved in determining the connections between cells and the matrix as mediated by hemidesmososmes Type II (Desmosomes on the other hand are cell-cell junctions). When PKCα or PKCδ phosphorylates β4 intergrin, hemidesmosomes disassemble and facilitate cell migration (due to loss of stable adhesion) **(**Rabinowitz *et al*., 2004; Alt *et al*, 2004).

MARCKS (Myristoylated Alanine-Rich C Kinase Substrate) is one of the first identified PKC substrates (Wu *et al*., 1982). This 87 kDa protein is a membrane-associated protein that also binds to actin cytoskeleton. Upon phosphorylation by PKC, MARCKS dissociates from the membrane and translocates to the cytosol. This process is believed to initiate cell movement in fibroblasts (Disatnik *et al*., 2004).

From what is known about PKC substrates to date, many are associated with the cytoskeleton whose dynamic changes triggered by PKC phosphorylation are involved in the mechanisms that drive cell adhesion and migration (Larsson, 2006). However, there is reason to believe that, in view of the pleiotropic actions of PKC, additional substrates will be found elsewhere in the cell. To address the question of PKC substrates, the present study harnessed an open-ended approach called the "Traceable Kinase Method" to identify novel substrates of PKC-α, δ and ζ and to compare their overall patterns of phosphorylation in MCF-10A cell lysates.

Identification of new PKC substrates by the Traceable Kinase Method

To identify intracellular substrates of PKC presents a challenging problem. All protein kinases

must bind ATP which serves as the phosphate donor. Because the ATP binding site is virtually identical in all protein kinases, their activity cannot be distinguished by their ability to bind and utilize ATP. The conserved nature of the ATP binding site in most protein kinases was exploited by Dr. K. Shokat from the University of California (San Diego) whose laboratory developed The Traceable Kinase Method (Shah *et al*., 1997; Ting *et al*., 2001; Shah and Shokat, 2002; Witucki *et al*., 2002). This chemical-genetic approach allows one to distinguish a protein kinase of interest from all other protein kinases by genetically engineering the ATP binding site so that it can bind an unnatural ("bulky") ATP. As a result, proteins phosphorylated by this mutant in the presence of the ATP analogue would be the direct substrates of that protein kinase (Liu *et al*., 1998). The Traceable Kinase Method entails making a single site mutation at the ATP binding site where the N^6-amino group of ATP contacts the enzyme. A large side-chain residue (typically Met or Ile) is replaced by a simpler side-chain such as hydrogen (Gly) or a methyl group (Ala). The newly enlarged ATP binding site in the mutant enables it to utilize an unnatural phosphoryl donor A*TP (*e.g.*, N^6-phenyl-ATP) which is an ineffective phosphoryl donor for all other protein kinases.

Following site-directed mutagenesis at the ATP binding site, the cDNA encoding an epitope-tagged mutant kinase is transfected into target cells. After expression and immunoprecipitation of the mutant kinase, it can be used as a reagent along with the ATP analogue (*e.g.*, N^6-phenyl-ATP) and co-immunoprecipitated protein substrates for *in vitro* phosphorylation. This experiment is conducted under detergent-free conditions that preserve protein-protein interactions. As a result, immunoprecipitation of the mutant kinase would

co-immunoprecipitate any high affinity protein substrates. When compared with the bands obtained with the wildtype enzyme, samples with the mutant kinase should result in bands whose phosphorylation can be attributed directly to the mutant protein kinase. Mass spectrometry analysis is used to identify potential protein substrates in the band(s).

To determine the site of mutation in the PKCα active site, the ATP binding domain of PKCα was aligned with that of v-Src (used by the Shokat group) and with the catalytic domain of cAMP-dependent protein kinase (PKA), which has a high degree of sequence homology with PKC and had been co-crystallized with ATP (Zheng *et al*., 1993).

PKCα	(412) R-L-Y-F-V-M-E-Y-V-N-G (423).
v-src	(333) P- I- Y-I-V- I- E-Y-M-S- K (343)
PKA	(115) N-L-Y-M-V-M-E-Y-V-P-G (125)

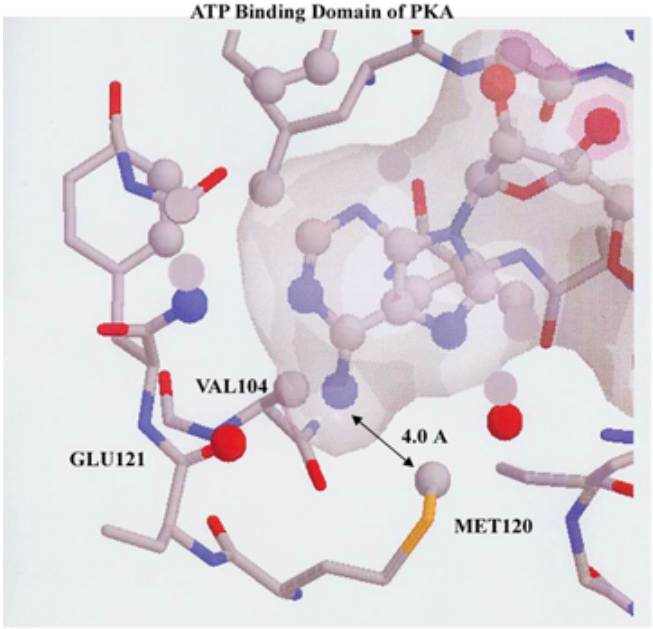

Figure 6. Crystal structure of PKA with bound ATP The model shows the three-dimensional structure of cyclic AMP-dependent protein kinase (PKA) with bound ATP in which the adenosine moiety is delineated by the translucent surface. The proximity of M120 to the adenosine moiety is illustrated. Molecular modeling was performed with Protein explorer (PDB entry 1ATP). (Abeyweera and Rotenberg, 2007).

Alignment of the primary sequence of PKA and v-Src revealed that Met-120 in PKA corresponds to I-338 in v-Src, the site modified by the Shokat laboratory. Met-120 was also identified in a three-dimensional structure of PKA (co-crystallized with ATP) as a sidechain in the ATP binding domain that is closely positioned to the N^6-amino group of adenosine (Abeyweera and Rotenberg, 2007). In both v-Src and PKA, the residue at this position comes within 5 Å of the N^6 amino of the adenosine of ATP. In PKCα, this site corresponds to Met-417 (M417). Mutants of PKCα were prepared in which M417 was substituted by either alanine (Ala) or glycine (Gly) (Abeyweera and Rotenberg, 2007). Despite the enlarged ATP binding cavity, the mutant forms were also able to utilize traditional ATP as substrate.

Figure 7. Phosphorylation of an artificial substrate (myelin basic protein) by WT-PKCα or M417A-PKCα with different N^6-ATP analogues. FLAG-PKCα plasmids (WT or M417A-PKCα) were transfected into MCF-10A cells and immunoprecipitated with anti-FLAG antibody. The immunopellets were aliquotted into Eppendorf tubes and used in a kinase reaction with myelin basic protein (MBP) plus non-radioactive 100 μM ATP analogue. ATP analogues consisted of (from left): N^6-phenyl-ATP, N^6-benzyl-ATP, N^6-phenethyl-ATP, and N^6-(3-methyl)-benzyl-ATP. The reactions were incubated at 30°C for 10 min, resolved by SDS-PAGE, and transferred to a PDVF filter. The membrane was probed with an antibody that recognizes phosphorylated PKC substrates. Protein standards consisted of non-phosphorylated MBP (MBP) and phosphorylated MBP (P-MBP).

When incubated with a protein substrate, namely myelin basic protein, and different ATP analogues, the traceable mutant M417A PKCα could utilize three of the four analogues present,

whereas the wildtype PKCα showed no reaction with any of the bulky analogues, as shown in Figure 7 (Abeyweera and Rotenberg, 2007).

Because of the importance of PKC in cancer metastasis, it is essential to identify its substrates in order to understand the mechanisms underlying various cancerous phenotypes. These substrates would greatly facilitate the discovery of anti-cancer drugs and therapies. The following scheme shows an incomplete model of what is known of PKCα activities and their cellular consequences.

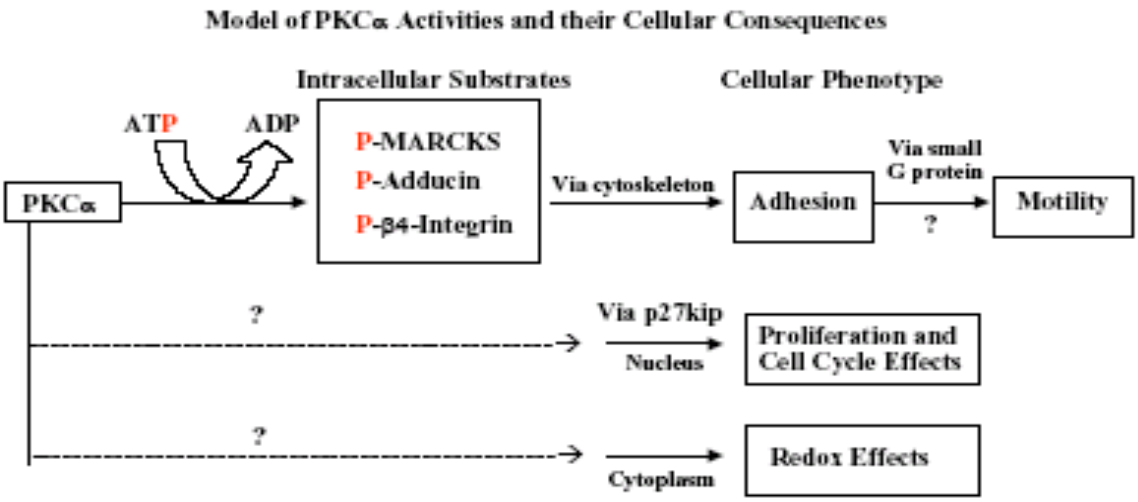

In the first project to be presented (Chapter 3), comparative phosphorylation profiles were determined for PKCα, δ and ζ, thus representing the conventional, novel and atypical isoforms, respectively, in MCF-10A cells using the traceable mutant of each isoform. The purpose was to identify potential substrates that co-immunoprecipitate with and undergo phosphorylation by each mutant kinase, as well as to determine the degree of overlapping specificity by these isoforms.

The Role of Myristoylated Alanine-Rich C Kinase Substrate (MARCKS) in Cell Motility

MARCKS is a known intracellular PKC substrate and its phosphorylation has been used as an indication of PKC activation. Phosphorylation of this protein by PKC occurs at four distinct sites (see below), that can be inhibited through competitive binding of Ca^{2+}/calmodulin to this segment in the protein. Four serine residues have been identified as phosphorylation sites recognized by PKC (Graff, *et al*., 1989) in the so-called effector domain:

$^{(150)}$ LysLysLysLysLysArgPheSerPheLysLysSerPheLysLeuSerGlyPheSerPheLysLysAsnLysLys $^{(174)}$

MARCKS interacts with anionic phospholipids in the plasma membrane through electrostatic interactions of the positively charged lysine residues within its effector domain and hydrophobic interactions of the N-terminal myristoyl group. As a result of phosphorylation, the electrostatic interactions are disrupted, leading to the release of the protein from the membrane. Following its release, phospho-MARCKS is cycled back via microtubules and is returned to the membrane as MARCKS, presumably upon dephosphorylation by PP1 and PP2A, two protein phosphatases that are known to act on phospho-MARCKS (Clarke *et al*., 1993) and to be associated with microtubules (Meisinger *et al*., 1997). During the interval that MARCKS is not associated with the membrane, actin cytoskeleton undergoes rearrangement. Binding of MARCKS with Ca^{2+}/ calmodulin during Ca^{2+} signaling also triggers the release of MARCKS into the cytoplasm while masking the phosphorylation domain. However, the downstream effect of Ca^{2+}/calmodulin binding to MARCKS is not well established.

Actin filaments of the cytoskeleton of B16 melanoma cells are known to be critical to membrane protrusion at the leading edge during cell movement, while retraction of the trailing edge is associated with microtubule dynamics (Ballestrem, *et al*., 2000). When bound with MARCKS, actin filaments are bundled into a rigid complex that is believed to maintain cell shape. Upon phosphorylation of MARCKS by PKC and its dissociation from the actin cytoskeleton, actin filaments reassemble and initiate the cell protrusion step. The association of MARCKS with actin filaments inhibits cell migration, presumably by preventing actin rearrangement. MARCKS has been reported to be associated with the platelet-derived growth factor receptor in human hepatic stellate cells and its over-expression could inhibit cell migration stimulated by PDGF in these cells (Rombouts *et al*., 2008). However, when a siRNA reagent was used to specifically knock-out membrane-bound MARCKS, cell migration was greatly enhanced in the presence of PDGF (Rombouts *et al*., 2008). This finding confirms the model in which membrane-bound MARCKS crosslinks actin and inhibits migration. MARCKS has also been shown to be associated with dynamic adhesions and to stabilize them in highly motile melanoma cells (Pfenninger *et al*., 2009). These studies established a role for MARCKS at the membrane and cytoskeleton. As a direct PKC substrate, MARCKS is known to be involved in cell migration and adhesion through its association with the cytoskeleton but the activities of phospho-MARCKS in the cytoplasm have not been further documented. Nonetheless, evidence of phospho-MARCKS in cells is an intracellular indication that PKC is catalytically active.

The interest in MARCKS arose from the fact that it is directly phosphorylated by PKC and it is associated with migration activity. While its function in the membrane has been extensively studied, the possibility that it serves an additional role in the cytoplasm has not been explored. Upon its phosphorylation by PKC in fibroblasts (Allen and Aderem, 1995), MARCKS associates with lysosomes prior to its return to the membrane via microtubules. However, the specific significance of the phospho-MARCKS-lysosome interaction was not investigated further, nor was it reported to be correlated with cell motility. In the second project to be described (Chapter 4), phospho-MARCKS is examined for its role in the motility of mouse melanoma cells, B16 F1 and F10. The two related cell lines have differing metastatic potential in a syngeneic model (C57BL/6 mice). F1 cells are not metastatic and are weakly motile *in vitro*, whereas F10 cells are metastatic in mice and are highly motile *in vitro* (Gopalakrishna and Barsky, 1988).

The work described here investigated PKC substrates on the motility pathway in cancer cells. The findings shed light on the underlying mechanisms of cancer metastasis and provide potential targets for future anti-cancer drug design.

CHAPTER 2

MATERIALS AND METHODS

Materials. MCF-10A cells were obtained from The Barbara Ann Karmanos Cancer Center (Detroit, Michigan). B16 F1 and F10 mouse melanoma cells were obtained from Memorial Sloan Kettering Cancer Institute, and A375 and WM 278 human melanoma cells were purchased from ATCC. DMEM/F12, RPMI 1640 cell media, fetal calf serum, DNA sequencing primers, Alexa fluor antibodies and pCDNA3.1 vector were obtained from Invitrogen (Carlsbad, CA). DMEM, EMEM and a plasmid encoding α6-tubulin were purchased from ATCC (Manassas, VA). FLAG antibody (M2), the pCMV4 vector and the Quik-Change Mutagenesis kit were purchased from Stratagene (La Jolla, CA). Anti-FLAG EZ-view beads, mouse monoclonal α-tubulin antibody (DM1A), nocodazole and phosphatase inhibitors cocktail were acquired from Sigma-Aldrich (St. Louis, MO). MARCKS and phospho-MARCKS rabbit monoclonal antibodies were obtained from Epitomics (Burlingame, CA), phospho-PKC substrate antibody was purchased from Cell Signaling Technology, Inc. (Beverly, MA), and the shRNA-encoding plasmids were from Origene (Rockville, MD). Mouse monoclonal GFP antibody, PKCε C-terminal antibody, horseradish peroxidase-conjugated secondary antisera, radioimmune precipitation buffer (RIPA buffer) and protein A/G agarose beads were obtained from Santa Cruz Biotechnology (Santa Cruz, CA). PKCε N-terminal antibody was purchased from BD Biosciences, and the pCR3-ε-tag plasmid encoding wildtype PKC-ζ was a gift from Dr. M.G. Kazanietz (University of Pennsylvania). Fugene 6 transfection reagent was obtained from Roche Applied Science (Indianapolis, IN), and PolyExpress DNA transfection reagent was purchased from InnoVita, Inc. (Gaithersburg,

MD), and the chemiluminescence reagent (Supersignal West Pico) was obtained from Pierce Co. (Rockford, IL). Immobilon-P transfer membranes and mouse monoclonal anti-myc antibody were purchased from Millipore Corp. (Bedford, MA). Calphostin C, *bis*-indoleylmaleimide and Go6976 were acquired from EMD Biosciences Inc., (La Jolla, CA). ATP analogues (phenyl-ATP, benzyl-ATP, phenethyl-ATP and 3-methylbenzyl-ATP) were obtained from Axxora (San Diego, CA). The DAG-lactone reagent (JH-131E-153) was a gift from Dr. V. Marquez (NCI-Frederick, NIH) and was the pure R-enantiomer contained in the previously reported racemic mixture (Garcia-Bermejo *et al*., 2002).

Cell culture and transfection. B16 F1 and F10 cells were cultured in 10-cm plates in RPMI 1640 medium supplemented with 10% fetal calf serum, 1% of penicillin/streptomycin and 0.1% of fungizone. MCF-10A cells were cultured in DMEM/F12 medium supplemented with 5% fetal calf serum, 2% penicillin/streptomycin, 0.2% fungizone. Cells were incubated at 37^{o}C with 5% CO_2 and split twice per week (F1 cells), or once per week (MCF-10A cells). Human melanoma A-375 cells were cultured in DMEM supplemented with 10% fetal calf serum and 1% penicillin/streptomycin, and WM-278 cells were cultured in 2% Tumor Medium. Cells were re-plated one day prior to transfection so that the cell density was 60-70% on the day of the experiment. Cells were washed with PBS and cultured in serum-free growth medium prior to transfection. Plasmid DNA was mixed with Fugene 6 transfection reagent in a 1:2 ratio (m/v). For 10-cm plates, 6 μg of plasmid DNA was mixed with 12 μl Fugene 6 and incubated for 30 min at room temperature. The mixture was added to cells in serum-free medium and incubated at 37^{o}C with 5% CO_2. After 6 h, complete medium was restored to the cells and

incubation continued overnight. For cells transfected with Fugene 6, the efficiency was 50-60%. The shRNA-encoding plasmid (5 μg for 60 mm plate) was prepared with PolyExpress DNA transfection reagent in a ratio of 1:3 (μg shRNA/μl reagent) in serum-free medium. The reagent was added to cells in 2.8 ml complete medium and the cells were incubated for 72 h at 37^{o}C (5% CO_2). The bi-cistronic shRNA encoding plasmid (Origene) co-expresses the shRNA product and red fluorescent protein (RFP), therefore providing a means by which to assess transfection efficiency. For F1 cells transfected with the PolyExpress reagent, efficiency was judged to be 80% or higher.

Transformation of bacterial cells and plasmid preparation. Plasmid DNA was diluted to approximately 50ng/μl. Competent DH5α cells were gently thawed on ice and 50 μl cells were transferred to a pre-chilled Eppendorf tube. One microliter of the diluted DNA was added to the bottom of the cells and the mixture was incubated on ice for 30 min. After subjecting the cells to heat-shock for 45 sec at 42^{o}C, the mixture was incubated on ice for another 2 min. Pre-warmed (to 37^{o}C) S.O.C medium (0.9 ml) was added to the mixture and incubated in a water bath shaker for 1 h at 37^{o}C at 200 rpm. The reaction medium (250 μl) was spread on an agar plate prepared with the appropriate antibiotic. The plate was incubated in a 37^{o}C incubator for over 16 h. Single colonies were isolated and cultured for subsequent plasmid preparation. Plasmids were isolated from bacterial cells by use of the Midi-prep kit (Qiagen, Valencia, CA).

Site-directed mutagenesis and construction of myc-tagged α6-tubulin. The plasmid DNA template was mixed with the reagents from the Quik-Change kit (Stratagene) plus two custom synthesized mutagenesis primers (Invitrogen) at the appropriate concentrations. All forward primers are shown in Table 1. The mutagenesis PCR cycle parameters were set as instructed by the manufacturer. After PCR, 1 μL of Dpn-1 restriction enzyme was added to the PCR product and the mixture was incubated for 1 h at 37^{o}C. One μl of the digested product was used to transform 50 μL Blue-script super-competent cells. The plates were incubated at 37^{o}C for 24 h and five colonies were analyzed for presence of the plasmid. The cDNA insert in each plasmid was detected by restriction digestion. To verify the presence of the mutation, cDNA sequence analysis of the entire open reading frame was performed on two or more clones (Macrogen, Inc., Rockville, MD).

Mutant	Primer
PKCδ-M427A	5'–AAG GAC CAC CTG TTC TTT GTG GCG GAG TTC CTC AAC GGG GGG GAC C-3'
PKCζ-I330A	5'–CGG TTG TTC CTG GTC GCG GAG TAT GTC AAT GGC GGG-3'
GFP-A2G_N/S-MARCKS	5'–CTT TGT TGA AGA CCA GCA TGG CCG CCC AGT TCT CCA AGA CCG C-3'

Table 1. Oligonucleotide primers used for site-directed mutagenesis.

For preparation of the A2G_N/S mutant of GFP-MARCKS, a second mutation (Gly → Ala) was introduced into N/S-MARCKS at the site of myristoylation (Gly-2) in order to prevent

acylation. The resulting double mutant (A2G_N/S-MARCKS) was constructed by a standard PCR approach (Quik-Change) using a primer in which the mutated bases are underlined as shown in Table 1. The sequence was confirmed by DNA sequencing of the entire open reading frame (Macrogen Inc., Rockville, MD).

Human α6-tubulin constructs (prepared by T.P. Abeyweera) were subcloned from a pCMV4 vector into the pCDNA3.1-myc vector (Invitrogen) so as to confer a myc tag on each construct. cDNA constructs for the wildtype α6-tubulin, the pseudo-phosphorylated mutant (S165D) and the phosphorylation-resistant mutant (S165N) were amplified from a pCMV4 vector by a standard PCR method with engineered 5' BamHI and 3' XbaI sites. The amplified fragment was inserted into a pCDNA3.1 vector at these restriction sites. The entire sequence was verified by DNA sequencing (Macrogen Inc.). Protein expression of myc-tagged constructs was verified by Western blot analysis using a rabbit polyclonal anti-myc antibody (Millipore Corp.).

Immunoprecipitation. Cells were lysed in hypotonic, detergent-free buffer [20mM Tris pH 7.4, 2 mM $MgCl_2$, 2 mM EGTA and 1 mM dithiothreitol (DTT)] containing protease inhibitors (1 mM phenylmethanesulfonyl fluoride, 10ng/mL leupeptin, and 10ng/mL soybean trypsin inhibitors) and phosphatase inhibitors. Sixty microliters of EZview-FLAG beads (pre-equilibrated in cold PBS) were added to 500 μl lysate and rotated for 2 h at 4^oC. The beads were centrifuged at 8200 x g for 30 sec and washed twice with 500 μl PBS and a third time with 500 μl kinase buffer (50 mM Tris, 12 mM magnesium acetate, 1 mM EGTA and 1

mM DTT). For immunoprecipitation of soluble α-tubulin, the soluble fraction was prepared as follows: MCF-10A cells were collected and pelleted by centrifugation for 5 min at 1000 x g. Cells were lysed in 0.2 ml microtubule stabilization buffer (0.1 M PIPES, pH 6.9, 30% glycerol, 5% (v/v) DMSO, 1mM $MgSO_4$, 1mM EGTA, protease inhibitors and phosphatase inhibitors) for 20 min at room temperature. After centrifugation for 45 min at 100,000 x g at 25^{o}C to remove membranes and polymerized tubulin, the supernatants (which contained soluble tubulin) were transferred to fresh tubes and normalized for total protein. The total volume was increased to 1 ml by adding RIPA buffer containing protease inhibitors and phosphatase inhibitors. Monoclonal anti-α-tubulin antibody (2 μg) (DM1A) was added to each lysate and immunoprecipitation was carried out at 4^{o}C with rotation. After 2 h, 40 μl of protein A/G beads suspension was added to each lysate and the incubation was continued for 1 h at 4^{o}C. The immunocomplex was pelleted by centrifugation at 3000 x g for 5 min and washed three times with 500 μl PBS prior to addition of 5X SDS sample buffer and heating for 5 min at 95^{o}C. For immunoprecipitation of myc-tagged α-tubulin mutants, cells were lysed in 500 μl RIPA buffer containing protease inhibitors and phosphatase inhibitors and 10μM *bis*-indoleylmaleimide-1 (BIM). After normalizing for total protein, the volume of each lysate was increased to 1 ml by adding RIPA buffer. Mouse monoclonal anti-myc antibody (8 μg) was added to each lysate and immunoprecipitation was carried out overnight, as described above.

Cell lysis and western blot. Samples of known protein concentration were denatured with 5X SDS sample buffer (50% glycerol v/v, 1% SDS, 0.05 % bromophenol blue, 0.4 M Tris pH 6.8,

and 2mM β-mercaptoethanol) which was diluted with the protein sample to a final concentration of 1X, followed by heating at 95^{o}C for 5 min. Samples were resolved by SDS-PAGE (typically 8% polyacrylamide) and electrophoretically transferred to a PVDF membrane (Millipore Corp.). The primary antibody was applied to the blot and incubated for 2 h at room temperature (or overnight at 4^{o}C as indicated) with shaking. After washing the membrane three times with TBST (0.9% NaCl, 20 mM Tris pH 7.4, 0.1% Tween 20 v/v), the appropriate secondary antibody (Santa Cruz Biotechnology) was added to the blot and incubated for 1 h at room temperature with shaking. After washing three times with TBST, the membrane was developed with the chemiluminescent reagent (Pierce Biotechnology, Rockford, IL).

ATP Analogue Assay. MCF-10A cells were transfected with wild-type (WT) PKCδ or PKCζ and the cells were lysed in hypotonic detergent-free buffer. WT PKCs (α, δ, or ζ) or the corresponding traceable mutant kinases were immunoprecipitated with EZ-view-FLAG beads (α or δ isoforms) or anti-PKCε (for PKC-ζ proteins). The immunopellets with bound WT or mutant enzyme were aliquotted to each of five Eppendorf tubes into which was added either ATP or the appropriate ATP analogue (phenyl-ATP, benzyl-ATP, phenethyl-ATP or 3-methylbenzyl-ATP). The reaction mixture consisted of 25 mM Tris pH 7.4, 0.5 mM EGTA, 10 mM magnesium acetate, 1 mM DTT with protease inhibitors and phosphatase inhibitors, 1mg/ml phosphatidylserine, 50 μg myelin basic protein (MBP) and 100 μM ATP or ATP analogue was added to initiate the reaction (t = 0). To stimulate PKCδ, 10 μM DAG-lactone was added to the reaction mixture, whereas PKCζ stimulation was produced with 1 μM

ceramide. The reaction was carried out for 10 min at 30^{o}C and quenched by adding 5X SDS sample buffer. The samples were heated for 5 min at 95^{o}C and analyzed by SDS-PAGE. The best analogue for each mutant was determined by assay of MBP phosphorylation by Western blot using the phospho-PKC substrate antibody.

For determination of protein phosphorylation profiles, WT PKCα and PKCδ and their corresponding traceable mutants were expressed in MCF-10A cells, and their lysates were prepared in hypotonic, detergent-free buffer, as described above. Phenyl-ATP (100 μM) was added to each pellet containing 5 μM DAG-lactone, PS (10 μg/ml), kinase buffer and 1 mM DTT. The reaction was carried out for 1 h at 30^{o}C and quenched by adding 5X SDS sample buffer followed by heating at 95^{o}C for 5 min. Samples were loaded onto a 7.5% SDS-PAGE gel, transferred to a PVDF membrane and developed using rabbit polyclonal phospho-PKC substrate antibody as the primary antibody.

Motility assay. In motility assays, cells (2 x 10^{6} per ml) were plated on a glass slide with small wells. The cells were applied to a 10-well slide through a cell sedimentation manifold (CSM Inc.), thereby ensuring that the cells sedimented as a tight concentric circle in each well. After incubation for 16 h at 37^{o}C, the manifold was removed and each image was recorded for the cells at the t = 0 time point. By taking images at a later time point (typically 6 h) (Motic Image 2.0 software), the increased area occupied by the cells was an indication of their motility. For some experiments that entailed addition of a reagent at t = 0 (e.g. DAG-lactone or okadaic acid), the specific details are indicated in the corresponding figure legends. Each condition was

carried out in triplicate wells and the results were averaged.

Immunocytochemistry and confocal microscopy. For B16 cells transfected with a plasmid that encodes a GFP fusion protein, cells were seeded onto cover slips at 24 h post-transfection and each coverslip was placed in a 6-well tissue culture plate and incubated overnight at 37^{o}C. Each coverslip was washed twice in 2 mL PBS and the cells were fixed for 10 min with 4% paraformaldehyde in 1X PBS (diluted from 10% paraformaldehyde in 10X PBS) and mounted in DABCO.

For immunocytochemistry of microtubules, cells were first incubated with microtubule stabilizing buffer (80 mM PIPES, 1 mM $MgCl_2$, 4 mM EGTA, 0.5% Triton-X100) for 30 sec and then fixed in -20^{o}C methanol for 3 min. Cells were treated with anti-α-tubulin (DM1A) antibody (1:400 dilution) for 30 min at 37^{o}C and washed three times with PBS containing 0.1% Trition X-100. Cells were treated with secondary antibody (Alexa Fluor 594 anti-mouse IgG) for 30 min, washed 3X with PBS with 0.1% Triton X-100 and mounted in DABCO.

Protein Identification by Mass Spectrometry. Identification of potential PKC substrate proteins in gel slices was performed at the Keck Foundation Mass Spectrometry Resource Laboratory at Yale Cancer Center. Gel-resolved proteins were digested *in situ* with trypsin (Promega) and batch-purified on a reversed-phase microtip, and resulting peptide pools were individually analyzed by liquid chromatography-tandem mass spectrometry on a Waters Q-TOF mass spectrometer, as previously described (Abeyweera and Rotenberg, 2007). All tandem mass

spectrometry spectra were searched using the automated MASCOT algorithm. Identification required that two or more spectra matched the same protein entry in the data base.

CHAPTER 3

Identification of PKC-α, δ and ζ substrates in human breast cells and characterization of α6-tubulin as a PKC substrate.

The first project in this chapter utilized the traceable kinase method with PKC-α, δ and ζ and successfully identified several potential substrates in MCF-10A human breast cells by MS-MS analysis. Two protein substrates, namely ROCK-1 and Cdc42-EP4, were analyzed as potential substrates.

In the second project, a novel PKCα substrate, namely α6-tubulin, was examined in human breast cells to map its phosphorylation site in cells. The stimulating role of α6-tubulin in motility upon PKCα phosphorylation was mediated by intact microtubules. These results completed a study previously begun by T.P. Abeyweera (T.P. Abeyweera, Ph.D. Dissertation, 2007) and were recently published (Abeyweera *et al*., 2009).

Preparation of the traceable kinase mutants of PKC-δ and ζ.

The objective of this study was to compare the phosphorylation profiles of the three distinct PKC members in MCF-10A cells and to identify potential substrate(s) of each enzyme. In addition to the conventional isoform PKCα, PKC-δ and ζ represent the novel and atypical PKC families, respectively. Their potential substrates could then be further analyzed for their effect on cancer phenotypes or tested as possible anti-drug targets.

Wildtype PKCδ cDNA was subcloned into a pCMV4A vector that conferred a FLAG tag during expression. PKCζ cDNA was contained in a pCR3 vector that conferred a PKCε tag. The PKCε tag was a short C-terminal sequence of PKCε fused to the N-terminus of PKCζ and proved to be useful in immunoprecipitation using an anti-PKCε antibody (Caloca *et al*., 1997). In order to locate the amino acid to be mutated at the ATP binding site to prepare the traceable mutants, sequences of PKC-δ and ζ were aligned with that of PKCα as follows:

PKCα	(412) R-L-Y-F-V-**M**-E-Y-V-N-G (423)	M417A
PKCδ	(422) H-L-F-F-V-**M**-E-F-L-N-G (432)	M427A
PKCζ	(325) R-L-F-L-V- **I** -E-Y-V-N-G (335)	I330A

The M417 mutation of PKCα was located by alignment with v-Src and PKA, as described in the Introduction (Chapter 1). The traceable mutant of PKCα had been prepared previously (Abeyweera and Rotenberg, 2007). Based on the sequence information for each isoform, M427A for PKCδ and I330A for PKCζ were made by site-directed mutagenesis. The mutations were confirmed by DNA sequencing (Macrogen USA, Rockville).

Characterization of PKC-α, δ and ζ mutants in MCF-10A cells.

The first step was to evaluate the expression levels of the traceable mutants. The traceable kinase of PKCα was previously well characterized (Abeyweera and Rotenberg, 2007). For PKC-δ and ζ, plasmids encoding WT or the corresponding mutant were transiently transfected into MCF-10A cells. Western blotting was performed to assess the expression level of the enzymes by use of either anti-FLAG (for PKCδ) or PKCε antibody (for PKCζ). As shown in Figure 8, PKCδ and PKCζ were stably expressed at a high level.

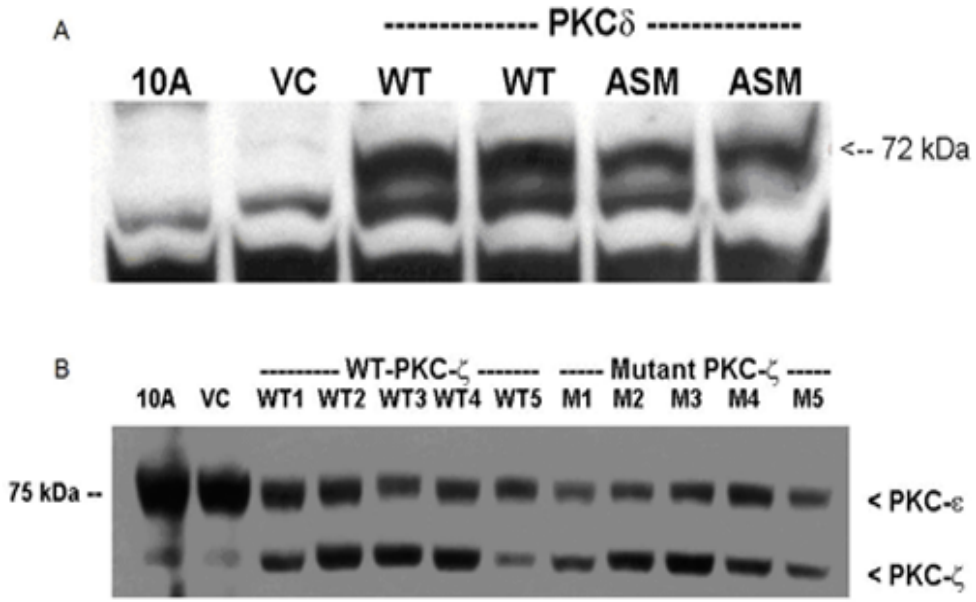

Figure 8. **Western Blot analysis of PKC-δ and ζ mutants.** (A) Wildtype (WT) and active site mutant (ASM) PKCδ were expressed as a 72-KDa band when compared to empty vector (VC) and parental cells (10A) and two clones of each were tested. (B) Wildtype (WT) and mutant (M) PKCζ were expressed as a 75-KDa band when compared to empty vector (VC) and parental cells (10A) and five clones of each were tested.

For PKCα, an important step to validate the intracellular function of the traceable mutant was to assay for its effect on motility. After transfection into MCF-10A cells, the traceable mutant of PKCα, also referred to as the active site mutant (ASM), was found to increase cell motility to the same level as the wildtype enzyme (Abeyweera and Rotenberg, 2007). This finding implied that the traceable mutant is competent to phosphorylate the same set of substrates in the cell that lie on the motility pathway. This approach was applied to the traceable mutants of PKC-δ and ζ as a means to validate their enzyme activities in the cell. As shown in Figure 9, PKCδ (WT and ASM mutant) increased motility by 7-fold and each activity was stimulated by DAG-lactone, a conventional and novel PKC activator. In contrast, the corresponding forms of PKCζ had no effect on motility and did not suppress the action of DAG-lactone which

stimulates only conventional and novel PKC isoforms.

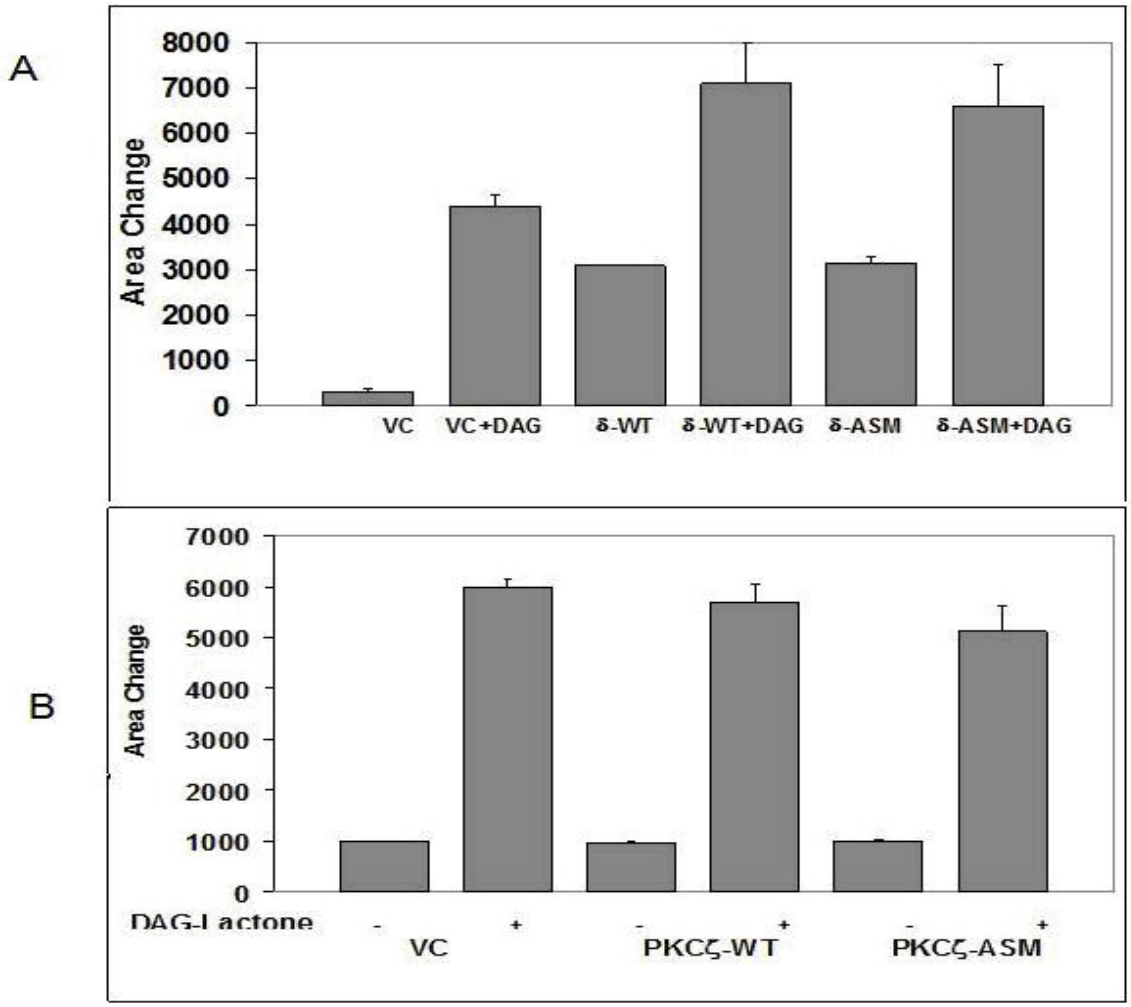

Figure 9: PKC-δ over-expression increases MCF-10A cell motility but PKC-ζ has no effect. (A) MCF-10A cells were transfected with VC (empty vector), δ-WT (PKCδ wildtype) or δ-ASM (PKCδ mutant) and were treated with or without DAG (DAG-lactone, a PKC activator) followed by motility assay as described in the Methods. (B) MCF-10A cells were transfected with VC (empty vector), PKCζ-WT (PKCζ wildtype) or PKCζ-ASM (PKCζ mutant) and assayed for motility as described in the Methods.

Isolation of the traceable kinase by immunoprecipitation.

One key aspect in the successful application of the Traceable Kinase Method was to utilize cells where very little PKC-mediated phosphorylation occurs (MCF-10A cells). Thus, immunoprecipitation of the traceable kinase is carried out under detergent-free conditions,

thereby promoting retention of high affinity (unphosphorylated) substrates at the substrate binding site. To facilitate this method, PKC-α and δ mutants were subcloned in a pCMV4A vector, which contained a FLAG tag for efficient immunoprecipitation with FLAG antibody. PKCζ was inserted in a pCR3 vector with a ε-tag, a short amino acid sequence of the C-terminus of PKCε. Even though PKCζ could be immunoprecipitated by anti-PKCε antibody, the fact that endogenous PKCε would also be precipitated posed a problem for downstream applications. To circumvent this difficulty, an extra immunoprecipitation step was adopted to pre-clear endogenous PKCε by using an anti-PKCε antibody directed against the N-terminus of wildtype PKC-ε. The two-step immunoprecipitation isolated PKCζ that was not contaminated with PKCε, as shown in Figure 10.

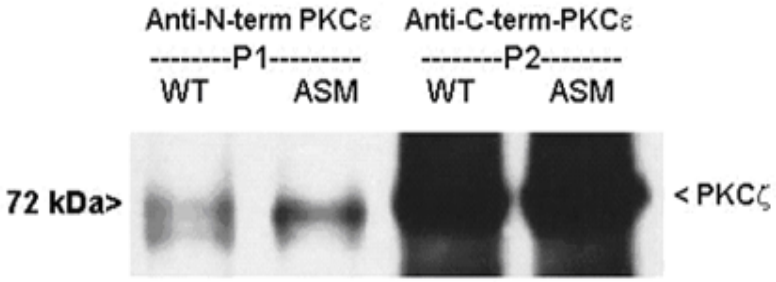

Figure 10. Isolation of PKCζ from MCF-10A cell lysates by immunoprecipitation. MCF-10A cells were transfected with either WT-PKCζ (WT) or the PKCζ mutant (I330A) and a two-step immunoprecipitation was performed using anti-N-terminal PKCε to pre-clear endogenous PKCε, followed by addition of anti-C-terminal PKCε antibody to immunoprecipitate ε-tagged PKCζ. The pellets were analyzed for PKCζ content by Western blotting using C-terminal PKCε antibody.

Selection of the appropriate ATP analogue for PKC-α, δ, and ζ mutants.

To utilize the traceable kinase mutants of PKC-α, δ and ζ for identifying potential substrates, it was important to select the appropriate ATP analogue that supported kinase activity of the traceable mutant but not that of the WT enzyme. The appropriate ATP analogue was

determined by performing kinase assays with myelin basic protein (MBP) as substrate and four commercially available ATP analogues that are all derivatives of the N^6 amino group of the adenosine moiety, as shown in Figure 11. It had already been demonstrated that the PKCα traceable kinase prefers N^6-phenyl-ATP to the other analogues (T.P. Abeyweera, Ph.D. Dissertation). Following immunoprecipitation of WT and mutant forms of PKC-δ or ζ, phosphorylation of MBP by these enzymes was carried out in an *in vitro* assay with each of the four ATP analogues or traditional ATP. Phospho-MBP was analyzed by Western blotting (shown in Figure 12) as a means to evaluate the preference of PKC-δ and ζ for one or more ATP analogues. Phospho-MBP was detected by Western blot with a commercially available primary antibody that recognizes the phosphorylated PKC consensus site (PKC phosphosubstrate antibody). The analogue that gave rise to the highest phospho-MBP levels in the mutant reaction but not in the wildtype reaction was selected as the appropriate ATP analogue. By this criterion, N^6-phenyl-ATP was chosen for use with each of the three PKC isoforms.

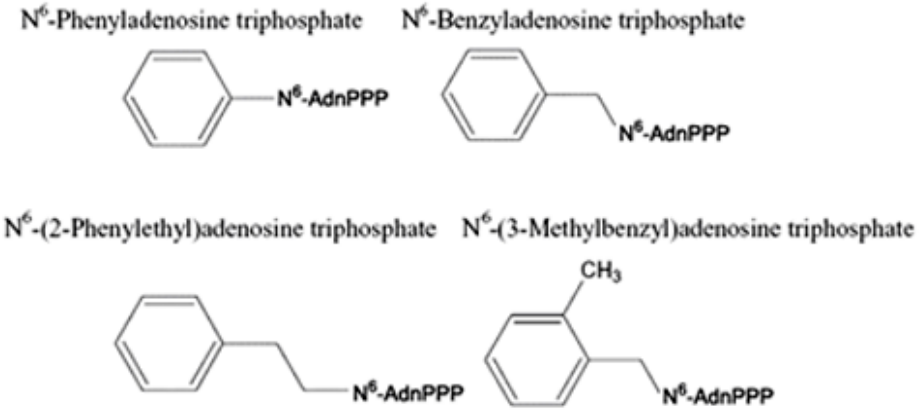

Figure 11: Commercially available ATP analogues.

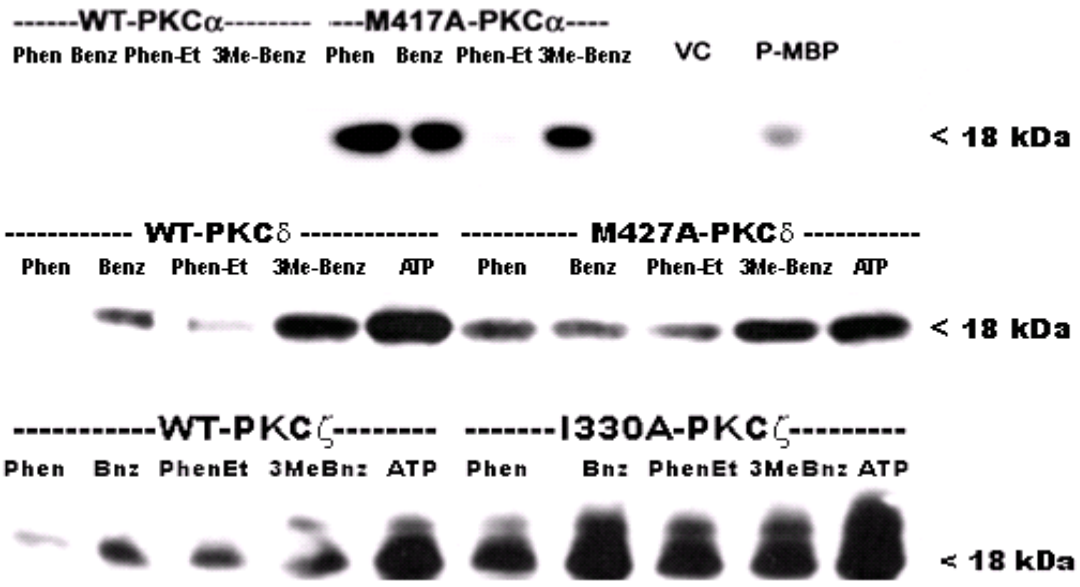

Figure 12. ATP analogue assays of PKC-α, δ and ζ. MCF-10A cells were transfected with the wildtype or mutant of PKC-α, -δ and -ζ. Determination of the preferred ATP analogue by each PKC isoform. Following immunoprecipitation of PKC-α and δ with FLAG antibody or of PKCζ with PKCε antibody, dephosphorylated MBP and an analogue of ATP (N^6-phenyl-ATP, N^6-benzyl-ATP, N^6-phenethyl-ATP, N^6-3-methyl-benzyl-ATP) or conventional ATP were added to the pellet. The reaction was carried out for 10 min for PKCα and 30 min for PKC-δ and ζ. Phosphorylation of MBP (18 kDa) was analyzed by Western blotting with the PKC-phospho-substrate antibody. (The results for PKCα were reproduced from T.P. Abeyweera, Ph.D. Dissertation 2007)

Comparison of the phosphorylation profile of PKC-α, δ and ζ in MCF-10A cells and identification of potential substrates.

To identify potential substrate(s) for PKC-α, δ and ζ in MCF-10A cells, the substrate co-immunoprecipitation method was used and followed by a kinase assay with the N^6-phenyl-ATP analogue. High affinity substrates bound to each of the three traceable kinases were phosphorylated using N^6-phenyl-ATP. The resulting phospho-protein bands were detected by Western blot with the PKC phospho-substrate antibody. The phosphorylation profiles of the three different PKCs were compared and are shown in Figure 13.

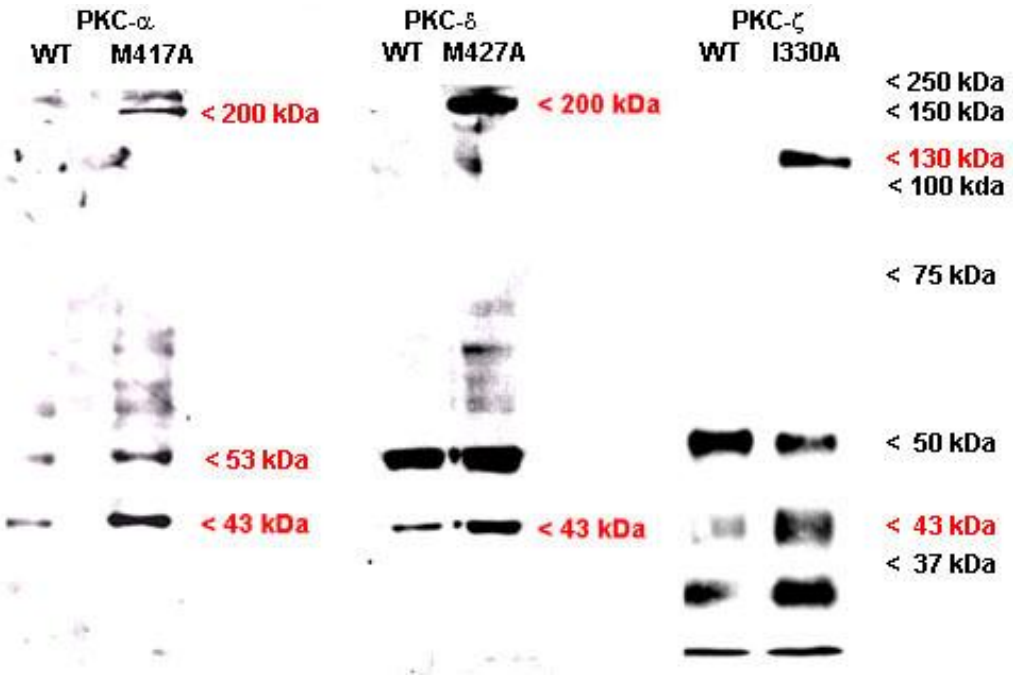

Figure 13. Phosphorylation profile of PKC-α, δ and ζ in MCF-10A cells. Cells were transfected with PKC-α, δ or ζ and following immunoprecipitation of the WT (wildtype) and mutant (M417A for PKCα, M427A for PKCδ and I330A for PKCζ), N^6-phenyl-ATP was added to the pellet. The reaction was carried out for 1 h at 30°C. Phospho-protein bands were resolved by duplicate 7.5% SDS-PAGE gels. The proteins on one gel were transferred to a PVDF membrane and PKC substrates were detected by Western blotting with the PKC phosphosubstrate antibody. The other gel was stained with Gelcode Blue and compared with the results of the first gel.

Mass spectrometry analysis of the bands produced exclusively by the traceable kinase PKC.

Phosphorylation of high-affinity substrates immunoprecipitated with the traceable kinase revealed several unique bands (discernable with Gelcode Blue stain) and were present exclusively in the mutant reaction. Several bands from the Gelcode Blue stained gels for the PKC-α and δ profiles and the 130-kDa in the PKCζ pattern were excised and evaluated by mass spectrometry (Keck Foundation at Yale University Cancer Center). A number of proteins were detected in each of the bands analyzed and a sampling is listed in Table 2. Some

PKCα
43 kDa: cdc42 effector protein-4, β-actin, VASP*
53 kDa: α- and β-tubulin, dynein-1, LIM protein
62 kDa: PAK2, desmoglein, MAPKKK7, Ras GTPase activating protein-binding protein,Hsp60, LIM protein-3
200 kDa: Rho-associated protein kinase (ROCK-1/2), IQGAP-1*, CLASP1, tensin-3, Rho/cdc42/Rac activating protein-1 (RICS), plectin* BCL-2-associated transcription factor, myosin

PKCδ
43 kDa: cdc42 effector protein-4, VASP*, desmoglein, β-actin, sphingomyelinase*
200 kDa: Rho-associated protein kinase (ROCK-1/2), IQGAP*, Rho/cdc42/Rac activating protein-1 (RICS), brefeldin A-inhibitor of GTP-exchange protein-2 (ARFGEF2), plectin (isoforms 1, 2), ARFGAP with Rho-GAP domain, MAP-4, CLIP-1, BCL-2-associated transcription factor

PKCζ
130 kDa: NAD(P) transhydrogenase

Table 2. **Proteins that co-immunoprecipitated with each traceable kinase and were identified by mass spectrometry.** Proteins that were previously known to be PKC substrates are indicated by an asterisk (*).

proteins were already known to be PKC substrates such as IQGAP (Grohmanova *et al*., 2004) and VASP (Chitaley *et al*., 2004), or PKC binding proteins such as plectin (Osmanagic-Myers and Wiche, 2004), thus validating the methods used here. It was noted that several proteins were GTP-dependent or GTP binding proteins, and three proteins are known to bind to microtubules (dynein) or plus ends of microtubules (CLASP, CLIP-1). High confidence values were assigned to ROCK-1 and Cdc42-EP4, two proteins contained in the 200-kDa bands for PKC-α and δ. In contrast to PKCα and PKCδ, PKCζ produced a very different phosphorylation pattern that included a strong band at 130kDa. This band contained very few proteins, one of which was NAD(P) transhydrogenase.

Testing of phosphorylation of ROCK-1 and Cdc42-EP4.

To determine whether ROCK-1 and Cdc42-EP4 are PKC substrates *in vitro*, recombinant proteins were obtained and tested for *in vitro* phosphorylation by pure recombinant PKCα and PKCδ using traditional ATP. As shown in Figure 14A, pure, recombinant ROCK-1 does not undergo phosphorylation with either PKCα or PKCδ. In addition, it was verified that ROCK-1 is not phosphorylated by PKC isoforms in cells treated with DAG-lactone. In this regard, following treatment of MCF-10A cells with either DMSO or DAG-lactone for 30 minutes, endogenous ROCK-1 was immunoprecipitated. The presence of phospho-ROCK1 in the pellet was analyzed by Western blotting using PKC phospho-substrates antibody, and compared with total ROCK-1 as determined using anti-ROCK1 antibody. In Figure 14B, ROCK-1 did not show enhanced phosphorylation after DAG-lactone treatment. In contrast with our findings with ROCK-1, Cdc42-EP4 proved to be a robust substrate of both PKCα and PKCδ *in vitro*, as shown in Figure 15.

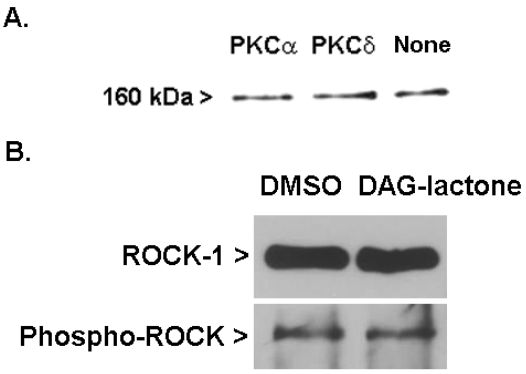

Figure 14. **In vitro and intracellular phosphorylation of ROCK-1.** (A) Pure recombinant ROCK-1 (100 ng) was incubated with pure recombinant PKC-α (170 ng) or PKC-δ (100 ng) and 100 μM ATP in kinase reaction buffer containing PS and DAG-lactone. The reactions were carried out at 30°C for 30 min and quenched by adding 5x SDS sample buffer. After heated for 5 min at 95°C, the samples were subjected to a 6% SDS-PAGE and probed with phospho-PKC-substrates antibody (1:1000). (B) MCF-10A cells were treated with 5μM DAG-lactone or DMSO (0.1% v/v) for 1 h and then lysed in RIPA buffer containing phosphatase inhibitors. Endogenous ROCK-1 was immunoprecipitated by a goat anti-ROCK-1 antibody (4μg per sample). The pellets were subjected to 6% SDS-PAGE. Parallel blots were developed with antibodies that specifically detected either ROCK-1 (1:200) or phospho-PKC-substrates (1:1000).

Figure 15. **In vitro phosphorylation of Cdc42-EP4 by PKC-α and PKC-δ.** Pure recombinant CDC42-EP4 (750 ng) was incubated with pure recombinant PKC-α (170 ng) or PKC-δ (100 ng) and 100 μM ATP in kinase reaction buffer containing PS and DAG-lactone (5μM). The reactions were carried out at 30°C for 30 min and quenched by adding 5x SDS sample buffer. After heating for 5 min at 95°C, the samples were subjected to a 7.5% SDS-PAGE and probed with phospho-PKC-substrates antibody (1:1000).

α6-Tubulin as a novel PKCα substrate.

Using the traceable kinase method, α6-tubulin, was recently identified by the Rotenberg lab to be a novel PKCα substrate (T.P. Abeyweera, Ph.D. Dissertation, 2007). To investigate the significance of the phosphorylation of α6-tubulin, site-directed mutagenesis of the four PKC consensus sites (Ser-158, Ser-165, Ser-241 and Thr-337) was employed. Namely, pseudophosphorylated (S→D) and phosphorylation resistant (S→N) constructs were prepared for each site. Motility assay revealed that only the S165D mutant gave rise to an elevated motility comparable to that induced by over-expression of wildtype PKCα after transient transfection. These experiments were performed by T. P. Abeyweera.

Demonstration that Ser-165 in α6-tubulin is the primary phosphorylation site.

Based on the motility assay, Ser-165 was thought to be a key site for PKC phosphorylation to downstream signaling. To demonstrate that Ser-165 was the *primary* phosphorylation site, a phosphorylation-resistant mutant, namely S165N was tested in MCF-10A cells. This site-directed replacement of Ser with Asn was chosen because Asn would serve as an isosteric control for the Asp used to generate the pseudo-phosphorylated mutant S165D. Upon preparation of S165N, its level of phosphorylation was judged by western blot using anti-α-tubulin, and was therefore could be compared directly with endogenous α-tubulin. Upon stimulation of MCF-10A transfectants with DAG-lactone, the expression of S165N mutant significantly suppressed phosphorylation of the endogenous α-tubulin, while cells transfected with the empty vector showed a high level of phospho-α-tubulin (Figure 16). The total α-tubulin level in these cells was not affected by the transfections.

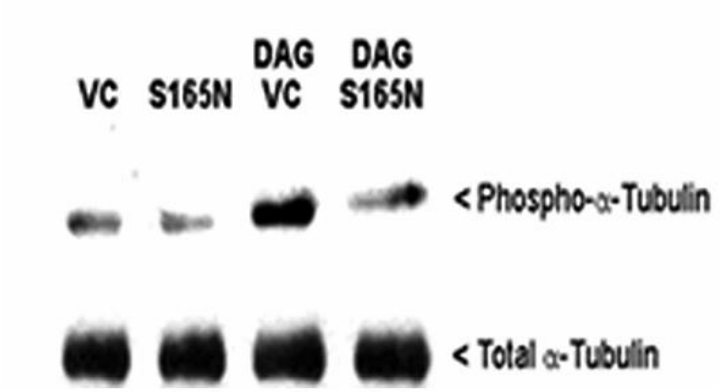

Figure 16. Phosphorylation-resistant α6-tubulin mutant (S165N) decreases phosphorylation of endogenous α-tubulin. GFP-S165N-α6-tubulin suppresses DAG-lactone stimulated phosphorylation of endogenous α-tubulin in MCF-10A cells. Cells were transfected with 4 μg of S165N mutant or the empty vector (VC; vector control). Identical transfectants were treated with 5 μM DAG-lactone or DMSO (0.1%, v/v) for 30 min at 37°C prior to lysis. Lysates were prepared in 0.2 ml of microtubule stabilization extraction buffer (0.1 M PIPES, pH 6.9, 30% glycerol, 5% DMSO, 1mM $MgSO_4$, 1 mM EGTA, and 1% Triton X-100) containing protease inhibitors and 10 μM BIM. A soluble fraction containing unincorporated tubulin was prepared from lysates (see "Methods") and normalized for total protein content (280 μg), and each sample volume was adjusted to 1.0 ml with radioimmune precipitation buffer. The samples were pre-cleared with mouse IgG agarose and immunoprecipitated with 2 μg of mouse anti-α-tubulin for 15 h with rotation at 4 °C. Immunopellets were divided into duplicate blots and probed in parallel with either rabbit polyclonal phospho-PKC substrate antibody (1:500 dilution) or rabbit anti-α-tubulin (1:2500 dilution).

When tested in other highly metastatic human breast cancer cell lines, such as MDA-MB-231 and MDA-MB-468 cells, the S165N mutant inhibited motility by 60-75% (T.P. Abeyweera, Ph.D. Dissertation, 2007; Abeyweera *et al.*, 2009). While MDA-MB-231 cells express a high level of PKCα (Gauthier *et al*., 2003), MDA-MB-468 cells do not have any conventional PKC isoforms (Mao *et al*., 2000) but express high levels of PKCδ, thereby suggesting that non-conventional PKC isoforms can also use α-tubulin as a substrate.

To investigate whether α6-tubulin could be phosphorylated by non-conventional PKCs, the wildtype, pseudophosphorylated and the phosphorylation-resistant α6-tubulin constructs were sub-cloned into a vector containing a C-terminal myc-tag that was used to efficiently immunoprecipitate the epitope-tagged protein. The expression level of these myc α6-tubulin constructs is shown in Figure 17.

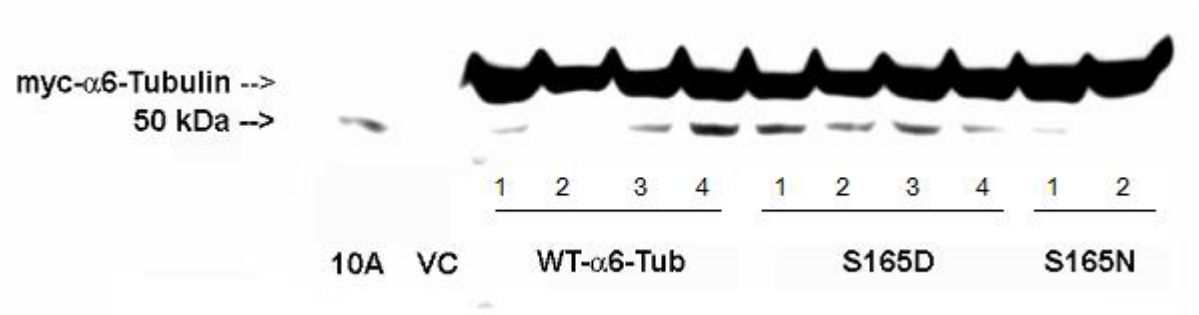

Figure 17. Expression of myc-α6-tubulin constructs. Cells were transfected with 4 μg of plasmid encoding WT, S165D or S165N. After 48 h of transfection, lysates were prepared in RIPA buffer containing protease inhibitors and 75 μg of total protein was loaded for SDS-PAGE. Myc-α6-tubulin was detected with rabbit myc antibody (1:1000 dilution) as a 55-kDa band.

Incorporation of myc-α6-tubulin mutant proteins into microtubules in MCF-10A cells.

To verify the expression of the myc-α6-tubulin constructs and to validate their function, confocal microscopy was performed to visualize the localization of each α-tubulin construct. As shown in Figure 18, the WT, S165D and S165N α6-tubulin proteins were equally incorporated into the microtubules in the cell.

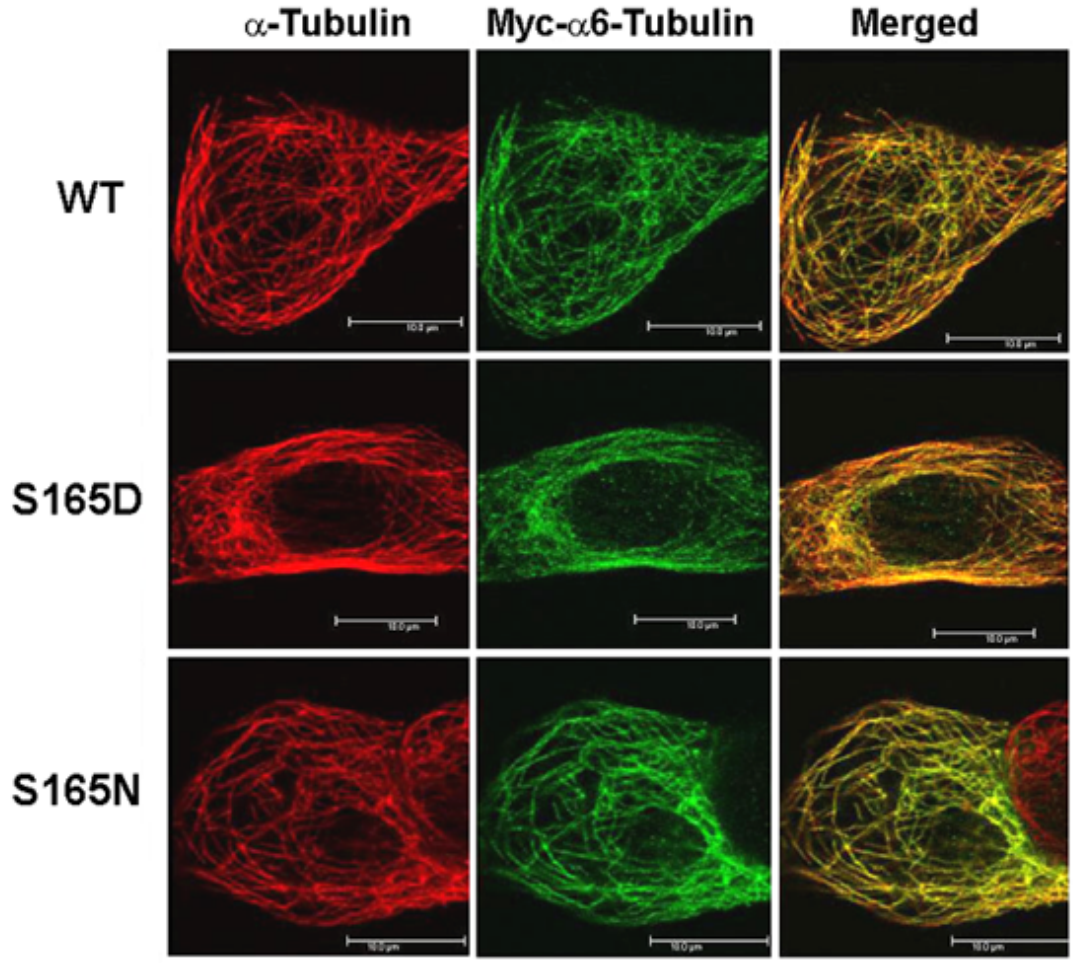

Figure 18. Incorporation of myc-α6-tubulin mutants into microtubules of MCF-10A transfectants. Cells transfected with WT-myc-α6-tubulin, or with either myc-S165N or myc-S165D mutants of α6-tubulin were extracted in microtubule stabilization buffer to remove unincorporated tubulin monomers prior to methanol fixation. By use of confocal microscopy, incorporation of myc-α6-tubulin was determined with a polyclonoal myc antibody (1:300) and a fluorescein-conjugated secondary antibody (Alexa fluor 488 at 1:400). Red fluorescent signals measured total α-tubulin incorporated into microtubules using α-tubulin monoclonal antibody (DM1A at 1:500) and rhodamine-conjugated secondary antibody (Alexa fluor 594 at 1:400). The results were qualitatively identical in at least two independent experiments and the images were representative of the cells viewed

The myc-tagged wildtype and S165N constructs were then transfected into metastatic human breast MDA-MB-468 cells which do not express any conventional PKC isoforms (Mao *et al.*, 2000). Phosphorylation of myc-tagged α6-tubulin (either WT or the S165N mutant) was assessed by Western blotting after immunoprecipitation of myc-tagged WT and S165N proteins

with a myc antibody. As shown in Figure 19, the WT reporter construct underwent substantial phosphorylation in MDA-MB-468 cells, as indicated by the intensity of the signal detected with the PKC substrates antibody. However, the phosphorylation-resistant mutant registered almost no phosphorylation signal, thereby signifying that S165 accounted for almost all of phosphorylation events occurring in α6-tubulin. Furthermore, phosphorylation of the myc-tagged WT reporter was almost entirely eliminated when cells were treated with 1 μM *bis*-indoleylmaleimide (BIM), a pan-PKC inhibitor, thus indicating that PKC was the sole source of kinase activity. Importantly, these results indicate that novel PKC isoforms and possibly atypical isoforms were the active kinases in these cells, and imply that α-tubulin can serve as a substrate for multiple PKC isoforms.

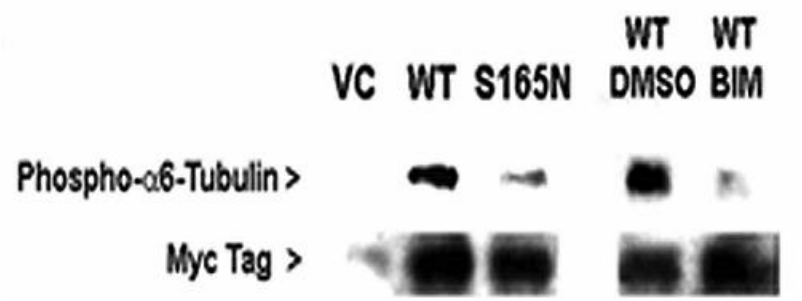

Figure 19. Phosphorylation of myc-tagged α6-tubulin reporter constructs in MDA-MB-468 cells. Cells were transfected for 48 h with 4 μg of plasmid encoding the myc-tagged WT α6-tubulin, S165N mutant, or VC. Where indicated, cells were treated with either 1 μM BIM or DMSO (0.1%, v/v) and incubated at 37 °C for 30 min prior to cell lysis. Whole cell lysates were prepared in 0.2 ml of buffer containing 50 mM Tris-HCl, pH 7.4, 150 mM NaCl, 1 mM EGTA, 10 μM BIM, and 0.5% Nonidet P-40. After normalizing for total protein content (550 μg), lysates were diluted 5-fold in detergent-free buffer, followed by pre-clearing with mouse IgG-agarose and immunoprecipitation with 5 μg of mouse anti-myc (6 h with rotation, 4 °C). Myc-tagged α6-tubulin (50 kDa band) was detected in a Western blot that was probed sequentially with rabbit anti-phospho-PKC substrates (1:500) and rabbit anti-myc (1:1000).

Motility induced by PKCα or S615D-α6-tubulin is microtubule-dependent.

The fact that α6-tubulin is a building block of microtubules suggests a relationship between this vital cytoskeletal component and the motility phenotype stimulated by the pseudo-phosphorylated α6-tubulin mutant. To address this question, a motility assay of MCF-10A transfectants was carried out with nocodazole, a microtubule destabilizing agent. In cells that had been transiently transfected with either wildtype PKCα or S165D, nocodazole almost completely blocked motility induced by either construct, as shown in Figure 20.

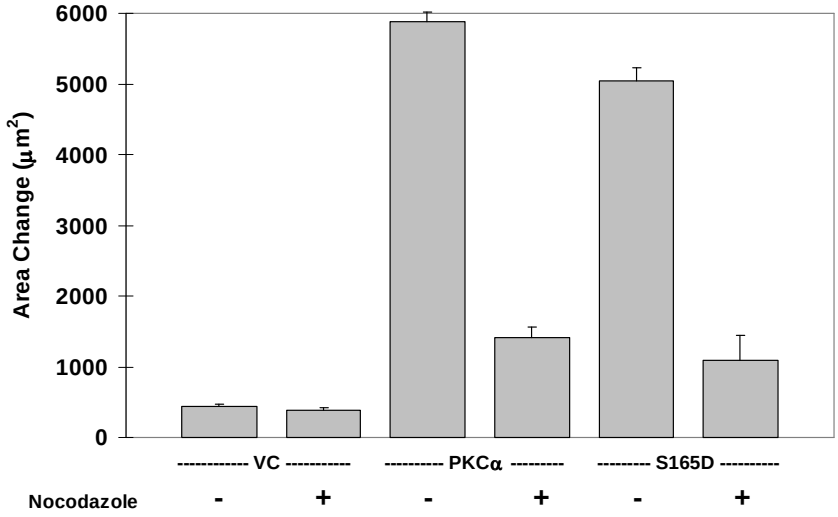

Figure 20. Motility of MCF-10A cells engendered by PKCα or S165D-α6-tubulin is eliminated by treatment with nocodazole. Cells were transfected with 4 μg of plasmid DNA encoding PKCα, myc-tagged S165D-α6-tubulin, or the vector control, as described under "Materials and Methods." After 48 h, cells were plated onto 10-well slides, and, following incubation at 37°C and 5% CO2 overnight, the cells were treated (*t* =0) with 5 μM nocodazole (or 0.1% (v/v) DMSO) and analyzed for motility after 8 h.

Effect of PKC activation on microtubule elongation.

To gain insight into the direct change in microtubule structures related to the elevated motility, a microtubule plus end binding protein called EB1 (Morrison *et al*., 1998; Vaughan, 2005) was expressed in MCF-10A cells as a GFP-fusion protein. The preferential binding of GFP-EB1

protein to microtubule plus ends was visualized by confocal microscopy as a means to assess whether microtubules were actively undergoing elongation. As shown in Figure 21, a dramatically higher GFP-EB1 binding to microtubules was observed in DAG-lactone treated cells, which implied that there were more actively growing microtubules upon PKC activation.

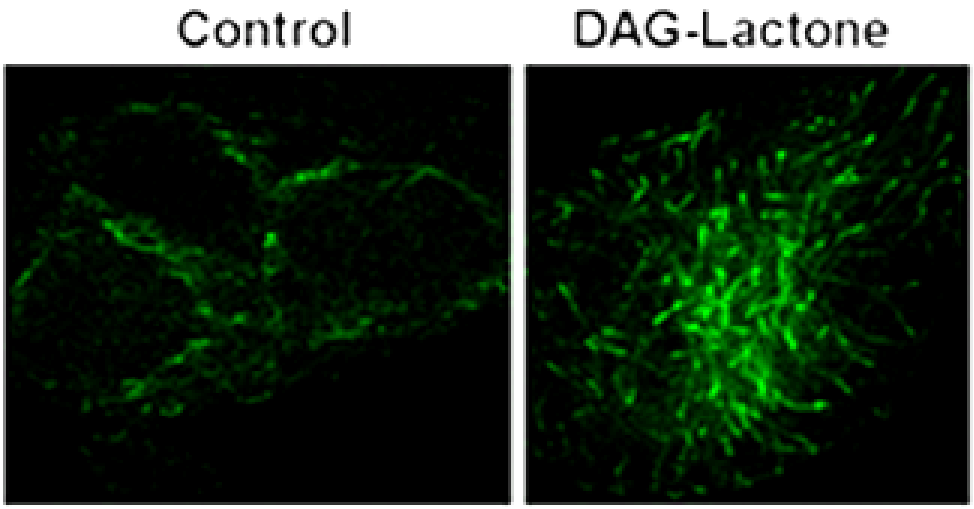

Figure 21. Confocal microscopy of MCF-10A cells transfected with GFP-EB1. Cells were transiently transfected with 4 μg plasmid DNA encoding GFP-EB1, followed by treatment with either 5 μM DAG-lactone or DMSO (0.1% v/v) for 30 min, and fixation in 4% paraformaldehyde, as described in the 'Materials and Methods'. Images were viewed under a Leica confocal microscope.

Discussion

In this study, a traceable kinase method that had been initially developed by Shokat and coworkers was used to identify PKC-α, δ and ζ substrates in human breast cells. In the wake of previous studies by the Rotenberg group in which a Shokat mutant of PKCα was developed at Met-417, similar mutants of PKC-δ and ζ were created by aligning the sequences of the three isoforms and performing site-directed mutagenesis at the residue that corresponded to Met-417 in PKCα. That alanine was chosen to be the small amino acid substitute was based on the

finding that M417A PKCα was superior to M417G PKCα when judged by their competence in reproducing the cell motility phenotype. M427A PKCδ was also able to reproduce the motility phenotype as the wildtype enzyme. This implies that the mutation in PKCδ did not hamper its recognition of substrates. Even though PKCζ did not show any effect on cell motility, there was no difference between the wildtype and mutant, nor did it interfere with the pro-motility effects induced by DAG-lactone which only activates conventional and novel forms, but not atypical PKC isoforms such as ζ.

There are four commercially available ATP analogues that are N^6-amino group derivatives. To select the appropriate bulky ATP analogue for PKCδ and ζ, an *in vitro* assay with MBP as the substrate was performed. The ability of each ATP analogue to support phosphotransferase activity of the mutant kinase was assessed by comparing MBP phosphorylation levels. The ideal ATP analogue was judged to be utilized only by the mutant kinase but not by the wildtype enzyme. Using this criterion, N^6-phenyl-ATP was selected for both PKCδ and PKCζ. It was noted that the wildtype enzymes of PKC-δ and ζ were able to use other ATP analogues to some extent, whereas the reactivity of PKCα with these analogues was restricted exclusively to phenyl-ATP. One explanation is that there are subtle structural differences in the δ and ζ isoforms that allow for greater flexibility in the ATP binding site.

Two strategies were proposed to identify potential PKC substrates in MCF-10A human breast cells. The first strategy was to express the traceable mutant and wildtype enzymes in MCF-10A cells and isolate them by immunoprecipitation. To the enzyme in the pellet were added

N^6-phenyl-ATP and a detergent-free cell lysate prepared from virgin MCF-10A cells. This design was carried out in order to react the enzyme with unphosphorylated substrates that were present in the lysate. The resulting phosphorylation banding pattern however had a high background for both wildtype and mutant reactions. A second strategy was pursued that focused entirely on the proteins that co-immunoprecipitated with the FLAG-tagged enzyme. This strategy was based on the assumption that since the immunoprecipitation medium did not contain any detergent, protein-protein interactions were preserved. As a result, it was thought that the enzyme would co-immunoprecipitate a number of high affinity substrates. The kinase reaction was initiated by addition of N^6-phenyl-ATP directly to the pellet containing co-immunoprecipitated substrates. This approach eliminated the high background and proved to be superior to the use of whole cell lysate as the substrate source.

In the current study, immunoblotting replaced autoradiography, which showed a strong background in the PKCα experiment (Abeyweera and Rotenberg, 2007). This non-radioactive method had low background and fewer bands (Figure 13) after probing the kinase reaction products with an antibody that recognizes the phosphorylated PKC consensus sequence. This method also narrowed the search for potential substrates and provided simpler manipulations. This study marked the first time that the Traceable Kinase Method was successfully coupled with a non-radioactive strategy to identify protein kinase substrates.

When the unique bands produced by the traceable mutants of PKC-α, δ and ζ were analyzed by mass spectrometry, several GTP-binding proteins and proteins known to be involved in

cytoskeletal structure were detected as potential substrates. The list, shown in Table 2, included proteins that bind small GTP-binding proteins (ROCK-1, cdc42EP4, Rho/cdc42/Rac-activating protein-1), as well as PKC substrates that had been previously documented by others *i.e.* IQGAP and VASP (Grohmanova *et al*., 2004; Chitaley *et al*., 2004), and by the Rotenberg laboratory *i.e.* α-tubulin (Abeyweera *et al.,* 2009)). The discovery of known PKC substrates validated the performance of the traceable kinases developed here. One identified protein, namely cdc42-EP4, could be verified as a substrate of PKCα and -δ by *in vitro* assays. Following construction of gain-of-function and loss-of-function mutants, it will be possible to evaluate the functional significance of these mutants in various phenotypes, including motility.

As a novel substrate identified by the Traceable Kinase Method, α6-tubulin was verified as an intracellular PKCα substrate whose phosphorylation reproduces the motility phenotype that the Rotenberg lab previous ascribed to PKCα in MCF-10A cells (Sun and Rotenberg, 1999). Motility assays revealed that a pseudophosphorylated mutant, namely S165D-α6-tubulin also stimulated MCF-10A cells motility. Furthermore, expression of a non-phosphorylatable mutant, namely S165N-α6-tubulin in MDA-MB-231 cells (which express abundant PKCα) and MDA-MB-468 cells (which express non-conventional isoforms) strongly inhibited motility of these cells (Abeyweera, Ph.D. Dissertation, 2007; Abeyweera *et al.*, 2009), as well as in DAG-lactone-stimulated MCF-10A cells. These findings implicated Ser-165 as the primary target of PKCα. It was further shown in the present work that the WT-α6-tubulin reporter was strongly phosphorylated, while myc-tagged S165N-α-tubulin was largely unphosphorylated. Because this result was detected in MDA-MB-468 cells, it was concluded that α-tubulin is also

a substrate for non-conventional PKC isoforms. It was noted that a small degree of phosphorylation did occur in the S165N mutant, suggesting that this site is not the sole phosphorylation site in α6-tubulin (Figure 19). In this regard, mass spectrometry of the pure, recombinant α6-tubulin that had been phosphorylated by pure, recombinant PKCα revealed that S158 is a site of phosphorylation. However, unlike Ser-165, the pseudo-phosphorylated mutant of S158 (S158D) had no effect on motility of MCF-10A cells (T.P. Abeyweera, Ph.D. Dissertation, 2007; Abeyweera *et al*., 2009). Thus, it appears that S165 is the only phosphorylation site that recapitulates the motile behavior engendered by PKCα.

The observation that PKC activation (by treatment with DAG-lactone) promotes microtubule elongation deserves further investigation (Figure 21). Whether PKC-engendered motility is correlated with the accompanying dynamic changes of microtubules remains to be defined. In this regard, elongating microtubules are believed to interact with small Rho GTPases (*e.g.* Rac1, Cdc42, and RhoA) that are often found at the leading edge of a moving cell (Nobes and Hall, 1995; Ladwein and Rottner, 2008). It is possible that stimulation of microtubule elongation by PKC-mediated phosphorylation of α-tubulin promotes cell motility through Rho GTPases. This model is supported by the finding that a Rac1 inhibitor NSC23766 could eliminate 80% of the motility induced by over-expression of the S165D-α6-tubulin mutant in MCF-10A cells (data not shown). This result was consistent with a previously finding that the dominant-negative form of Rac1 suppresses PKCα-stimulated MCF-10A cell motility, whereas the dominant-negative mutants of both Cdc42 and RhoA do not (Sun and Rotenberg, 1999).

CHAPTER 4

Study of Myristoylated Alanine-Rich C Kinase Substrate (MARCKS) in melanoma cells.

In this project, a known PKC substrate, namely MARCKS, was extensively studied to examine its role in the motility phenotype of B16 mouse melanoma cells. Most of the results presented here have been published (Chen and Rotenberg, 2010). For the first time, phospho-MARCKS was determined to have a cytoplasmic role in promoting motility. This finding offers a new avenue for identifying the binding partner(s) of phospho-MARCKS in the cytoplasm that may collaborate with MARCKS to propagate the motility signal.

Myristoylated Alanine-Rich C Kinase Substrate or MARCKS is a known PKC substrate that is associated with the plasma membrane through its N-terminal myristoyl moiety and an effector

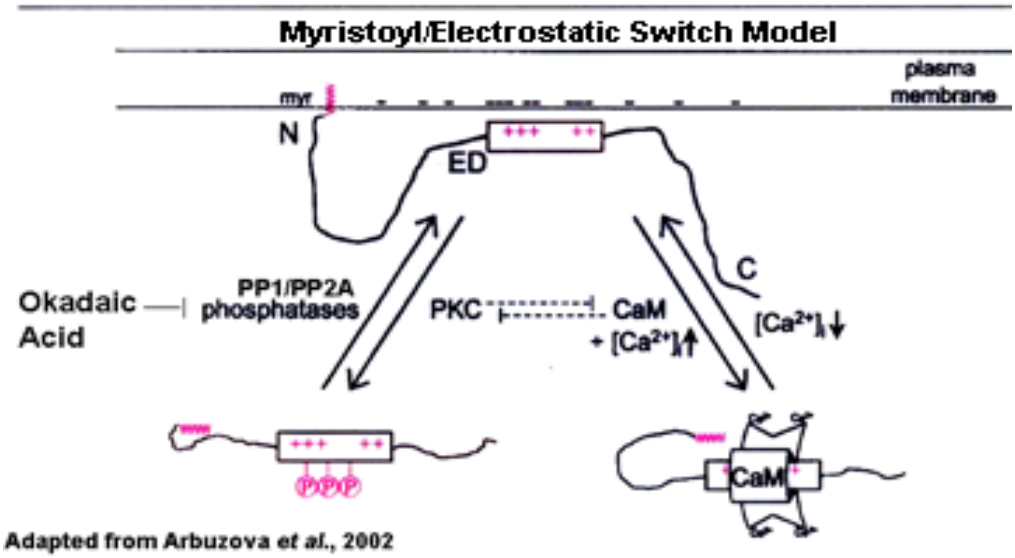

Figure 22. The myristoyl/electrostatic switch model of MARCKS. (Arbuzova *et al*., 2002)

domain that contains a cluster of positively charged amino acids and four serine residues, three of which are directly phosphorylated by PKC. MARCKS cross-links actin at the periphery of

the cell. Upon phosphorylation by PKC or binding to calmodulin, MARCKS translocates to the cytoplasm. The so-called myristoyl/electrostatic switch model is shown in Figure 22.

MARCKS expression and its phosphorylation state in mouse melanoma cells.

Two mouse melanoma cell lines, namely B16 F1 and B16 F10, were isolated from a syngeneic mouse model C57/BL6 (Fidler, 1973). F1 cells are non-metastatic, whereas F10 cells are highly metastatic (Gopalakrishna and Barsky, 1988). It was found that F10 cells, which are highly motile, express a high level of phospho-MARCKS (85 kDa band), while the less motile and non-metastatic F1 cells do not express detectable levels of this phospho-protein; however,

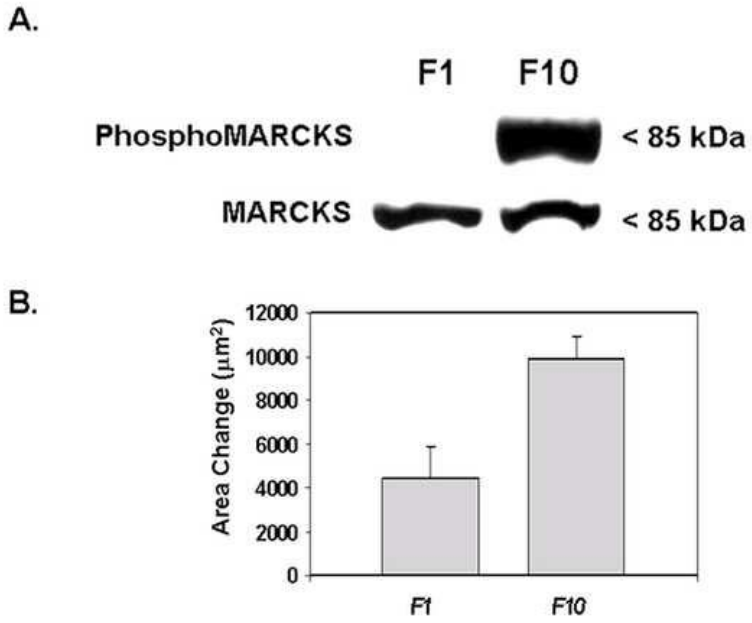

Figure 23. Phospho-MARCKS is elevated in murine melanoma cells having high motility. (A) Western blot analysis of B16 F1 and F10 cells was performed to determine endogenous expression of MARCKS and phospho-MARCKS. Cell lysates were prepared and resolved by SDS-PAGE (50 μg protein per lane) in duplicate gels, followed by transfer to PVDF membranes. The blots were developed with either anti-phospho-MARCKS (1:4000) or anti-MARCKS (1:1000). (B) Comparison of motility behavior of parental F1 and F10 cells was performed, as described in the 'Methods'.

both cell lines express equivalent levels of unphosphorylated MARCKS (Figure 23). This

finding correlated phosphorylation of MARCKS with motility in these melanoma cells, whereby F10 cells showed a 2.5-fold greater motility than F1 cells.

Constitutively active PKCα does not elevate levels of phospho-MARCKS.

The low phospho-MARCKS level and motility in B16 F1 cells was initially considered to be the result of low PKC activity. To test if this condition was the cause, a constitutively active

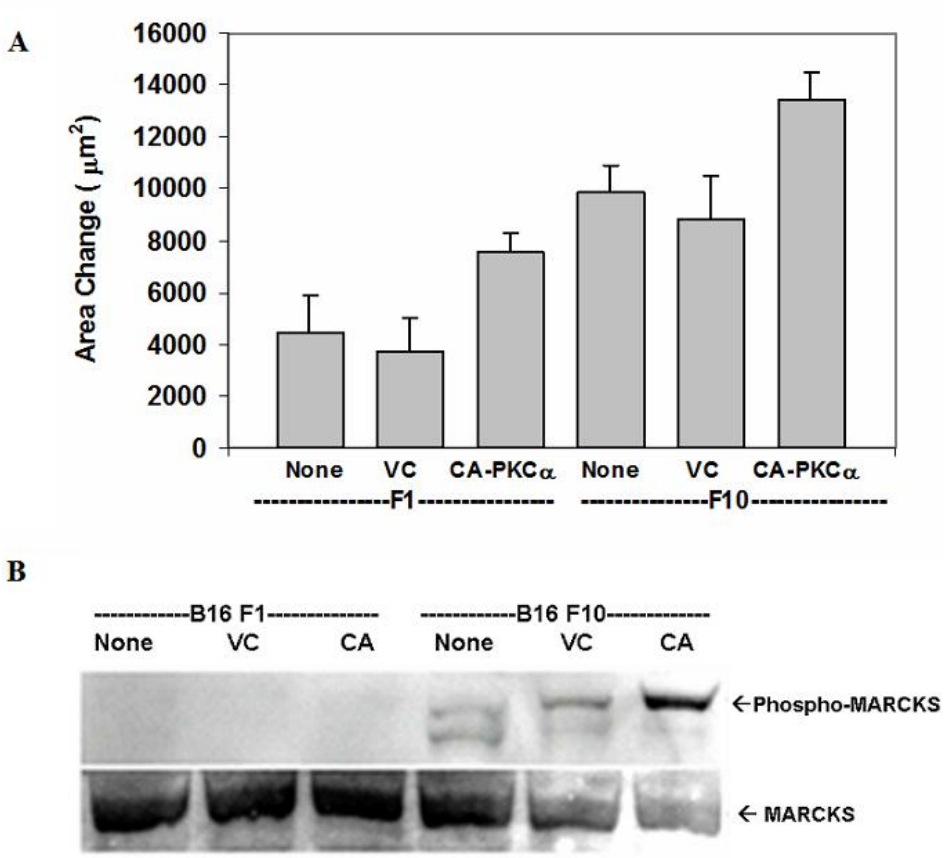

Figure 24. Effect of CA-PKCα on B16 cell motility and phospho-MARCKS levels. (A) Motility was measured following transient transfection of F1 cells and F10 cells with the control vector (VC) or CA-PKCα. Cell motility was measured after 6 h. All motility assays were carried out in triplicate. (B) Western blot analysis of F1 and F10 cells for expression of MARCKS. Cell lysates were prepared and applied to an 8% SDS-PAGE, followed by transfer to a PVDF membrane. The membrane was developed with either anti-MARCKS or anti-phospho-MARCKS and followed by a secondary antibody conjugated to HRP. Detection was by chemiluminescence.

PKCα (CA-PKCα) was overexpressed in both B16 F1 and F10 cells. Motility assays (Figure 24A) showed that CA-PKCα over-expression in B16 F1 cells stimulated motility by 50% but did not produce detectable phospho-MARCKS (Figure 24B). By contrast, there was a substantial increase in phospho-MARCKS level in B16 F10 cells (Figure 24B).

Okadaic acid treatment causes elevated phospho-MARCKS and motility in F1 cells.

Because F1 cells express abundant PKCα (Sanz-Navares *et al*., 2001), it was unexpected that they did not exhibit detectable phospho-MARCKS, especially following expression of CA-PKCα (Figure 24B) or after prolonged treatment with DAG-lactone (a membrane-permeable PKC activator) (Figure 25 top). Previous studies showed that

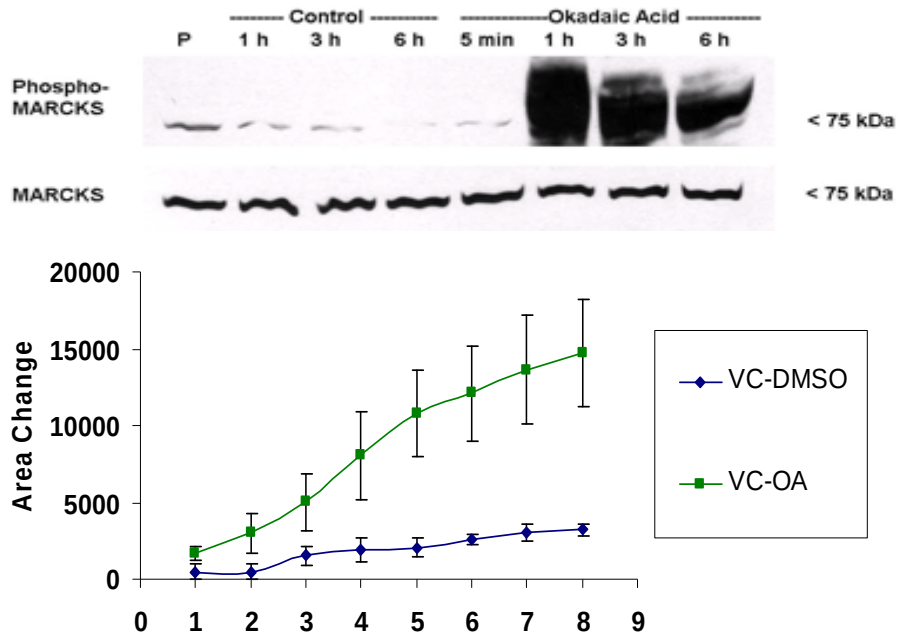

Figure 25. Time course study of the effect of OA on phospho-MARCKS and motility. (A) B16 F1 cells were treated with 1 μM OA or DMSO (control, 0.1% v/v) for 5 min, 1h, 3h or 6h prior to cell lysis in RIPA buffer containing phosphatase inhibitors. Lysates were subjected to 7.5% SDS-PAGE. Parallel blots were developed with antibodies that specifically detected either phospho-MARCKS (1:2000) or MARCKS protein (1:1000). (B) Motility of F1 cells was measured following treatment with 1 μM OA or DMSO (0.1% v/v) as vehicle control for the entire experimental period (8 h) The extent of movement was analyzed at 1 h intervals for a total period of 8 h. All motility assays were carried out in triplicate, as described in 'Methods and Materials'.

phospho-MARCKS undergoes dephosphorylation by PP1 and PP2A (Clarke *et al*., 1993) both of which can be inhibited by okadaic acid (OA). OA treatment of F1 cells produced a high level of phospho-MARCKS within 1 h and remained high for 6 h (Figure 25 top; 26A).

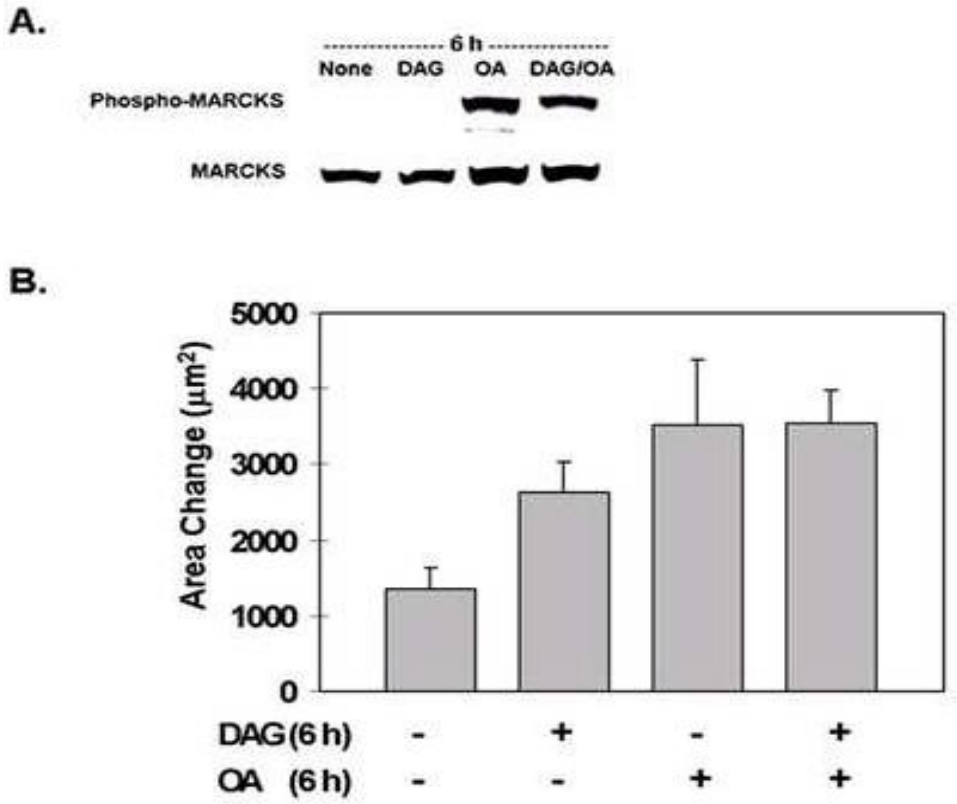

Figure 26. Okadaic acid-treated F1 cells exhibit dramatically higher levels of phospho-MARCKS and increased cell motility. (A) F1 cells were treated continuously with 5 μM DAG-lactone (DAG) and/or 1 μM okadaic acid (OA), or DMSO (0.1% v/v) for 6h. Lysates were prepared for Western blotting (100 μg/lane). Parallel blots were developed with antibodies that specifically detected either phospho-MARCKS (1:2000) or MARCKS protein (1:1000). (B) Parental F1 cells were plated in triplicate onto 10-well slides. Cells were treated with 5 μM DAG-lactone for continuous 6-h treatment with 1 μM OA (or DMSO (0.1% v/v). The extent of cell movement was analyzed for triplicate samples over a 6-h period and averaged.

OA treatment for up to 8h produced a dramatic increase in F1 cell motility from 353 μm^2/hr to 2004 μm^2/h (Figure 25, bottom). At 6 h post-treatment with OA, it was observed that addition of DAG-lactone produced no further increase on either phospho-MARCKS levels or cell

motility (Figure 26B). It was noted that even though DAG-lactone treatment did not increase phospho-MARCKS, it did elevate the motility to a small extent (Figure 26B). This result is consistent with DAG-mediated stimulation of PKC to interact with other target proteins that promote motility, but not membrane-level MARCKS protein.

PKC inhibition blocks phospho-MARCKS accumulation and motility stimulated by OA.

To investigate whether PKC was the major source of the phospho-MARCKS level produced by OA, a photo-activated membrane-selective PKC inhibitor, namely calphostin C (Liu *et al*., 1992) was applied to F1 cells prior to OA addition. Pretreatment of F1 cells with 1 μM calphostin C eliminated phospho-MARCKS and cell motility induced by OA, as shown in Figure 27. However, pretreatment with two other PKC inhibitors (*bis*-indoleylmaleimide and Go6976) at 1 μM did not eliminate phospho-MARCKS (data not shown).

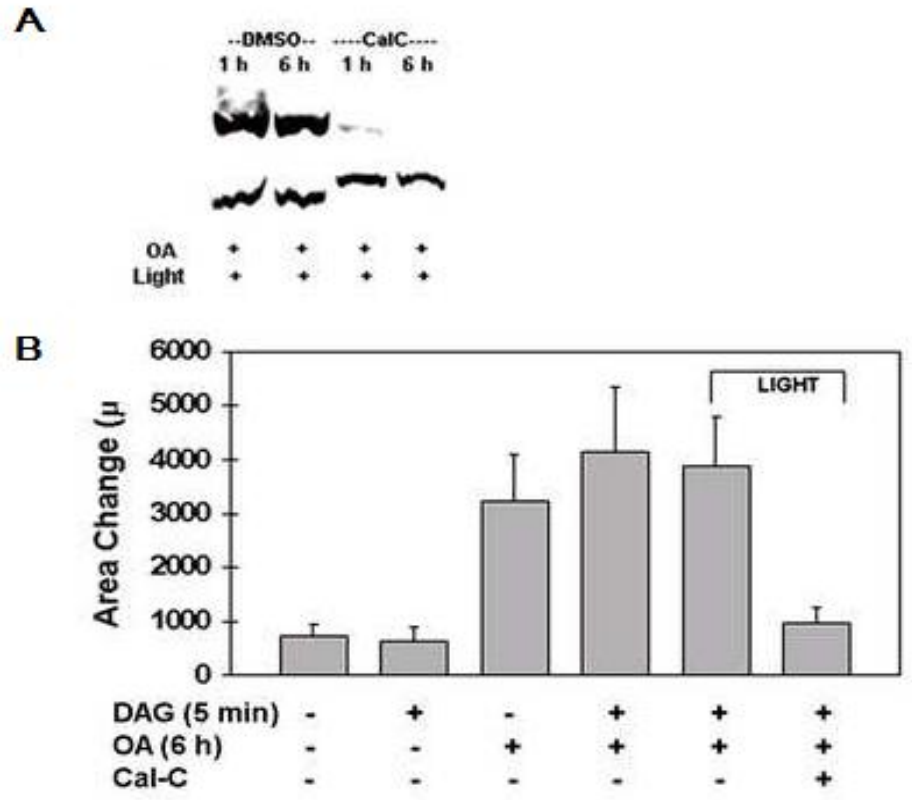

Figure 27. Calphostin C inhibits phospho-MARCKS accumulation and motility stimulated by OA. (A) A 10-cm culture plate containing F1 cells were treated with 1 μM calphostin C or DMSO (0.1% v/v) and placed on a fluorescent light box for 15 min, followed by 1 h incubation at 37°C (5% CO_2). The cells were washed twice with PBS and 5 ml complete medium was restored to the cells, followed by addition of 1 μM OA or DMSO (0.1% v/v) for 1 h or 6 h, as indicated. Lysates were prepared and duplicate Western blots (75 μg/lane) were developed with phospho-MARCKS (1:2000) or MARCKS antibodies (1:1000 dilution). The bands corresponding to MARCKS and phospho-MARCKS were at 85 kDa. (B) Parental F1 cells were plated in triplicate onto 10-well slides and treated with 5 μM DAG-lactone for 5 min (by wash-out with complete medium) and/or continuous 6-h treatment with 1 μM OA (or DMSO (0.1% v/v). Calphostin C (1 μM) or DMSO were added as indicated, as described in (A). The extent of cell movement was analyzed for triplicate samples over a 6-h period and averaged.

Phospho-MARCKS plays a major role in the motility phenotype produced by OA.

Because OA treatment traps a wide range of proteins in their phosphorylated state, it was essential to establish the specific contribution of phospho-MARCKS to F1 cell motility

induced by OA. A mouse MARCKS-specific shRNA vector was used to knock-down

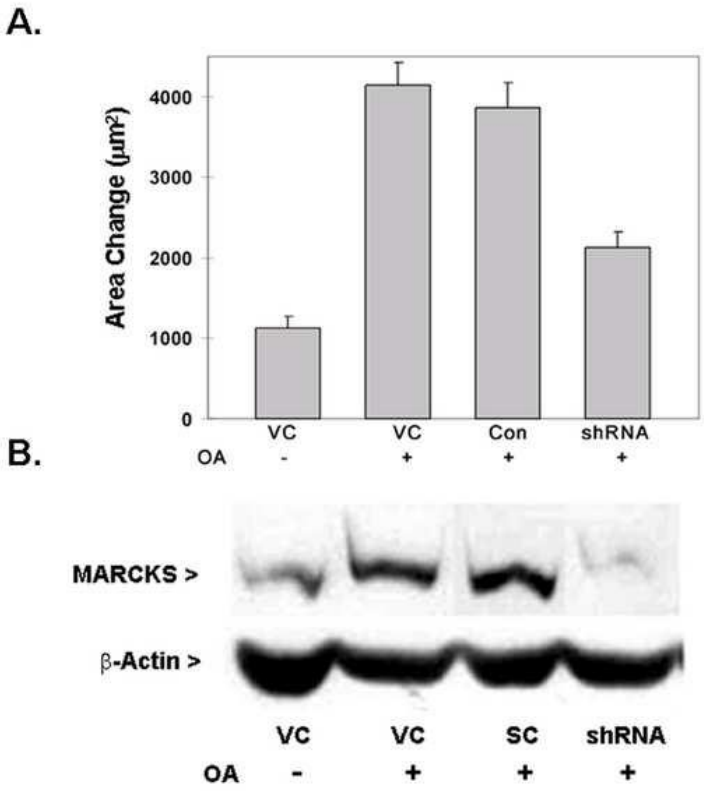

Figure 28. Knock-down of MARCKS in OA-treated F1 cells leads to decreased motility. Cells were transfected with plasmid DNA (5 μg) encoding mouse MARCKS shRNA, a scrambled shRNA control (SC or Con), or the empty vector (VC), as described in 'Materials and Methods'. Expression of MARCKS shRNA was coupled with co-expression of red fluorescent protein (RFP). At 55 h post-transfection, cells were re-plated in triplicate onto 10-well slides and incubated overnight at 37°C (5% CO_2). At 72 h post-transfection (t=0 for motility assay), cells were treated with 1 μM OA or DMSO (0.1% v/v) and incubated for 6 h at 37°C (5% CO_2). For measuring motility of fluorescent cells, images were recorded at t=0 and t=6 h (A). Alternatively, cells were lysed at 6 h post-treatment with 1 μM OA or DMSO (0.1% v/v), and lysates were analyzed by Western blot (75 μg/lane). (B). The blots were developed with anti-MARCKS (1:1000) and anti-β-actin (1:2000).

MARCKS prior to OA treatment. The use of a bi-cistronic vector that simultaneously expressed both the red fluorescent protein (RFP) and the shRNA product (as independent molecules) provided a convenient means to directly track the movement of fluorescent cells for assay of motility. Western blot analysis of the endogenous MARCKS level showed that there

was a nearly complete loss of total MARCKS protein following transfection of MARCKS shRNA as compared with the scrambled control shRNA and the empty vector (Figure 28B). Assay of OA-induced F1 motility of cells transfected with MARCKS shRNA resulted in inhibition by 66%; this value was calculated by correcting the motility of shRNA-expressing cells for the basal level of movement of cells transfected with the scrambled control (Con) and the empty vector (VC) (Figure 28A).

Expression of GFP-MARCKS mutants results in characteristic sub-cellular localization and motility effects in B16 F1 and F10 cells.

To further investigate the significance of phospho-MARCKS to motility, GFP-MARCKS mutants were used. The pseudo-phosphorylated (D/S) and phosphorylation-resistant (N/S) mutant constructs had all four PKCα mediated phosphorylation sites mutated to aspartate residues or asparagine residues, respectively (generously provided by P. Blackshear, NIEHS). An additional mutant, namely unmyristoylated-phosphorylation-resistant (A2G_N/S) was prepared by replacing a Gly residue (G2) of the phosphorylation-resistant mutant near the N-terminus with an alanine residue. This mutation disabled acylation at this site and subsequent membrane binding (Spizz and Blaskshear, 2001).

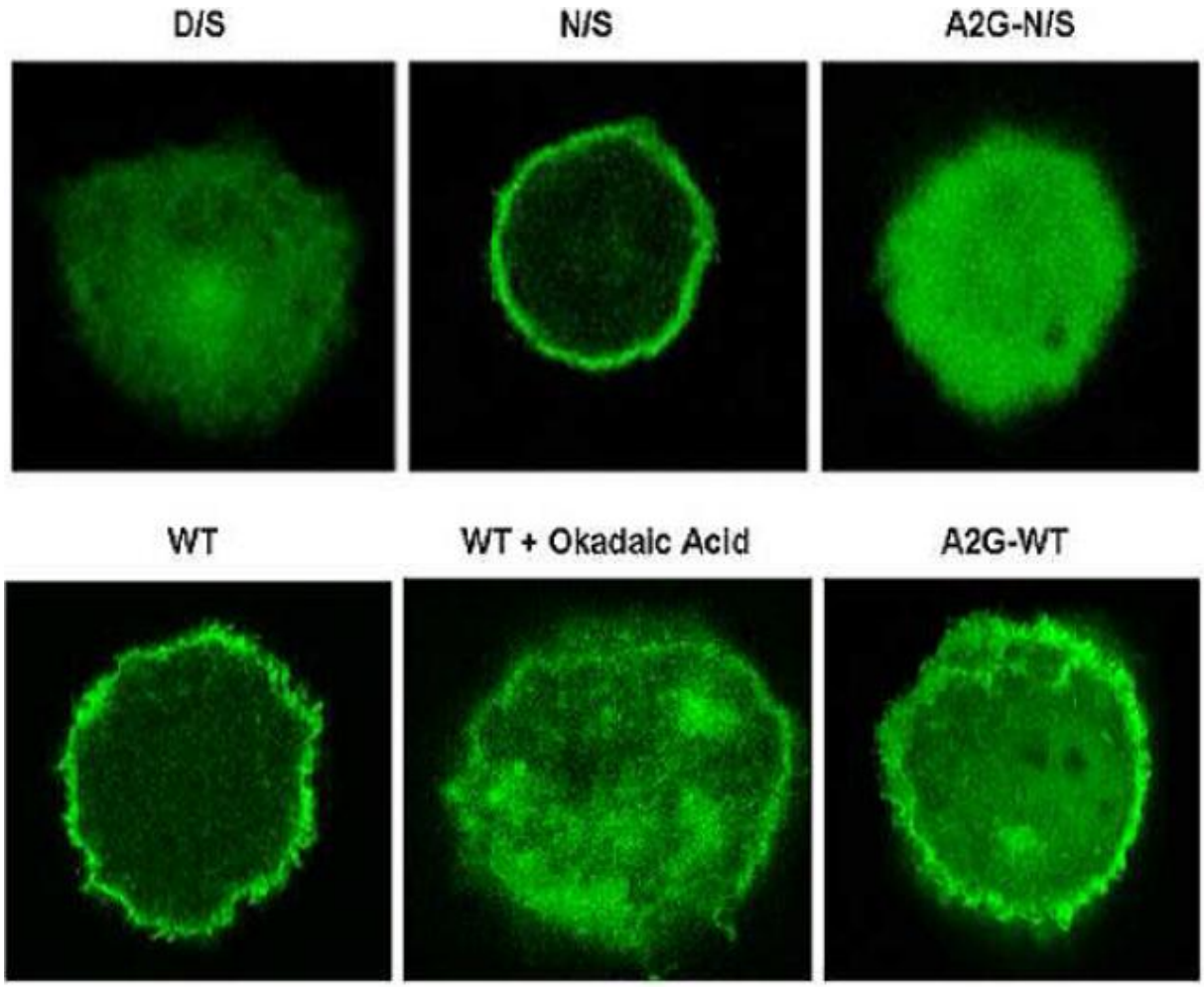

Figure 29. Confocal microscopy of F1 cells transfected with GFP-MARCKS mutants. Cells were transiently transfected with 4 μg plasmid DNA encoding pseudophosphorylated GFP-MARCKS (D/S), phosphorylation-resistant GFP-MARCKS (N/S), WT-GFP-MARCKS (WT), or unmyristoylated GFP constructs (A2G_N/S and A2G-WT). Cells expressing WT-MARCKS were treated with either 1 μM OA or DMSO (0.1% v/v), followed by fixation in 4% paraformaldehyde in PBS, as described in 'Materials and Methods' and viewed under a Leica confocal microscope.

The localization of the GFP-MARCKS mutants was examined after transfection into the cells, as shown in Figure 29. As predicted from the model for MARCKS, the pseudophosphorylated mutant was detected in the cytoplasmic compartment, whereas the phosphorylation-resistant mutant was found exclusively in the membrane. The wildtype GFP-MARCKS was localized primarily at the plasma membrane. However, in the presence of OA, wildtype GFP-MARCKS was detected in the cytoplasm within 1 h. This observation agreed with the finding that OA

maintains MARCKS in the phosphorylated state and consequently promotes the accumulation of MARCKS in the cytoplasm. The unmyristoylated-phosphorylation-resistant mutant was mainly localized in the cytoplasm due to the absence of the myristoyl group.

Over-expression of the GFP-MARCKS mutants and their effects on cell motility.

To establish the mechanistic significance of phospho-MARCKS to motile behavior in F1 and F10 cells, the appropriate gain-of-function (D/S) and loss-of-function (N/S) mutants were examined for their effects on motility. The expression levels of these GFP-MARCKS mutants were first demonstrated by Western blotting as shown in Figure 30. All GFP-MARCKS constructs were expressed at a high level. These constructs could be detected by both anti-MARCKS and anti-GFP antibodies as 100-kDa fusion proteins.

Figure 30. Western blot analysis of GFP-MARCKS expression. Western blotting with anti-GFP (1:500) or anti-MARCKS (1:1000) of whole cell lysates from F1 cells transfected with GFP-MARCKS constructs (20 μg/lane).

GFP-MARCKS expression level was much higher than endogenous MARCKS, which could only be detected when 10-fold higher total protein was tested by Western blot analysis. Expression of these GFP-MARCKS mutants resulted in dramatic changes in motile behavior of both F1 and F10 cells. In F1 cells the gain-of-function mutant (D/S) caused an elevated motility that was about 2.5-fold higher than that of parental cells (Figure 31 left panel). On the

other hand, the wildtype (WT) and loss-of-function mutant (N/S) had no effect in F1 cells. By contrast, in F10 cells, the D/S mutant achieved approximately a 2-fold higher motility, while the WT-GFP-MARCKS had a milder stimulating effect compared to control cells (VC). However, unlike F1 cells, the N/S mutant inhibited 70% of motility of F10 cells.

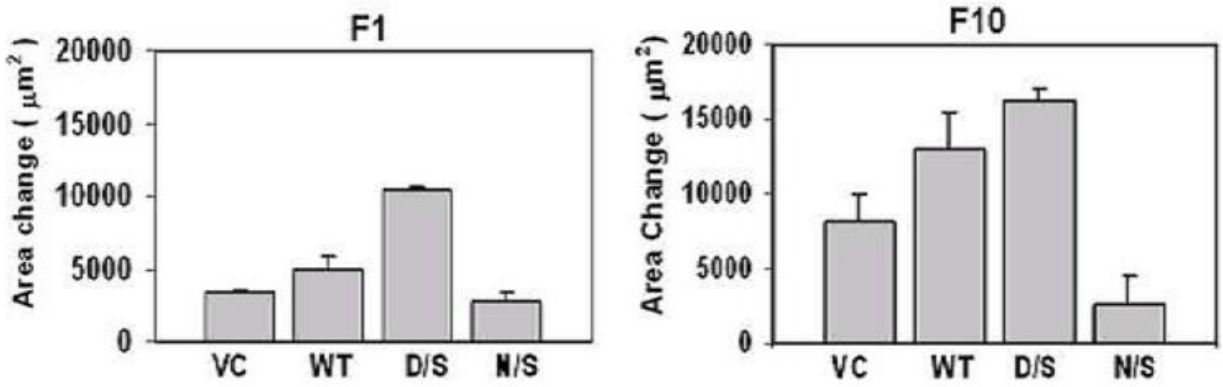

Figure 31. Motility behavior of B16 melanoma cells correlates with gain-of-function and loss-of function MARCKS mutants. Motility was measured following transient transfection of F1 cells (left panel), and F10 cells with the control vector (VC) or one of the following GFP-MARCKS constructs: wildtype (WT), pseudophosphorylated MARCKS (D/S); phosphorylation-resistant MARCKS (N/S).

In view of the stimulatory effect on motility by cytoplasmic pseudophosphorylated mutant (D/S), a role for phospho-MARCKS as a cytoplasmic factor in motile behavior was further explored. For this purpose, a double mutant (A2G_N/S) was developed that was both phosphorylation-resistant and cytoplasmic. When tested in F1 cells A2G_N/S mutant reduced cell motility induced by OA by 50% (Figure 32A). The same mutant also caused a decrease of intrinsic F10 cell motility by about 40% (Figure 32B).

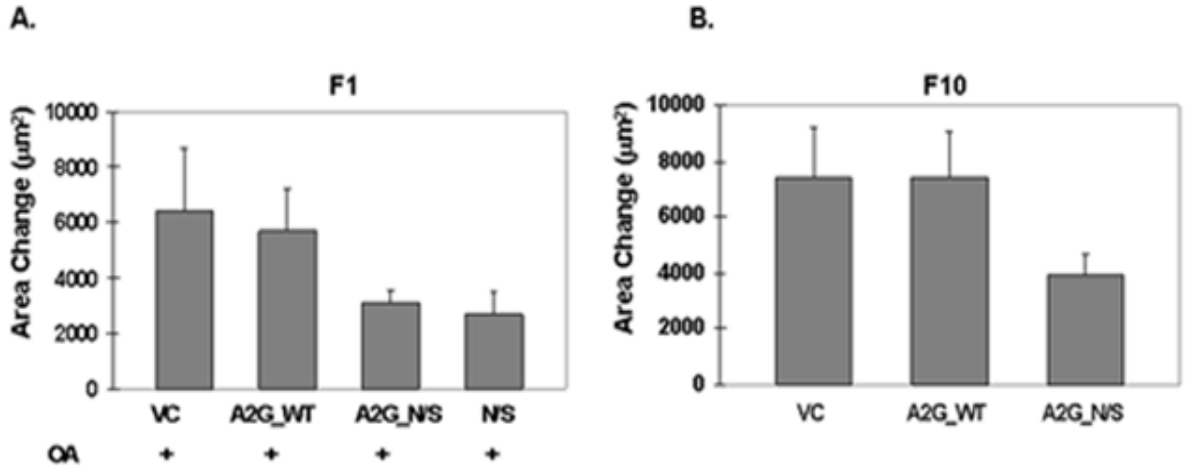

Figure 32. Motility of F1 and F10 cells transfected with phosphorylation-resistant mutants of GFP-MARCKS. (A) F1 cells were transfected with the unmyristoylated analogue A2G_N/S-GFP-MARCKS, N/S-GFP-MARCKS, WT-GFP-MARCKS, or the vector control (VC), followed by treatment with 1 μM OA for the entire experimental period (6 h). (B) Motility of F10 cells was measured following transfection with A2G_WT-MARCKS or A2G_S/N-GFP-MARCKS, or the vector control (VC). The extent of movement was analyzed after 6 h. All motility assays were carried out in triplicate, as described in 'Methods and Materials'.

It has been demonstrated by the Rotenberg lab that a pseudophosphorylated MARCKS mutant (DS-MARCKS) could stimulate MCF-10A cell motility, the same phenotype documented here for S165D α6-tubulin. Because α6-tubulin and MARCKS are both PKC substrates, it is tempting to speculate that the two substrates may act in concert downstream of PKC activation. The possibility that α6-tubulin and MARCKS participate in the same mechanism that drives motile behavior was further investigated.

Effect of S165N-α6-tubulin on cell motility stimulated by DAG-Lactone or OA.

The relationship between MARCKS phosphorylation and cell motility has been well

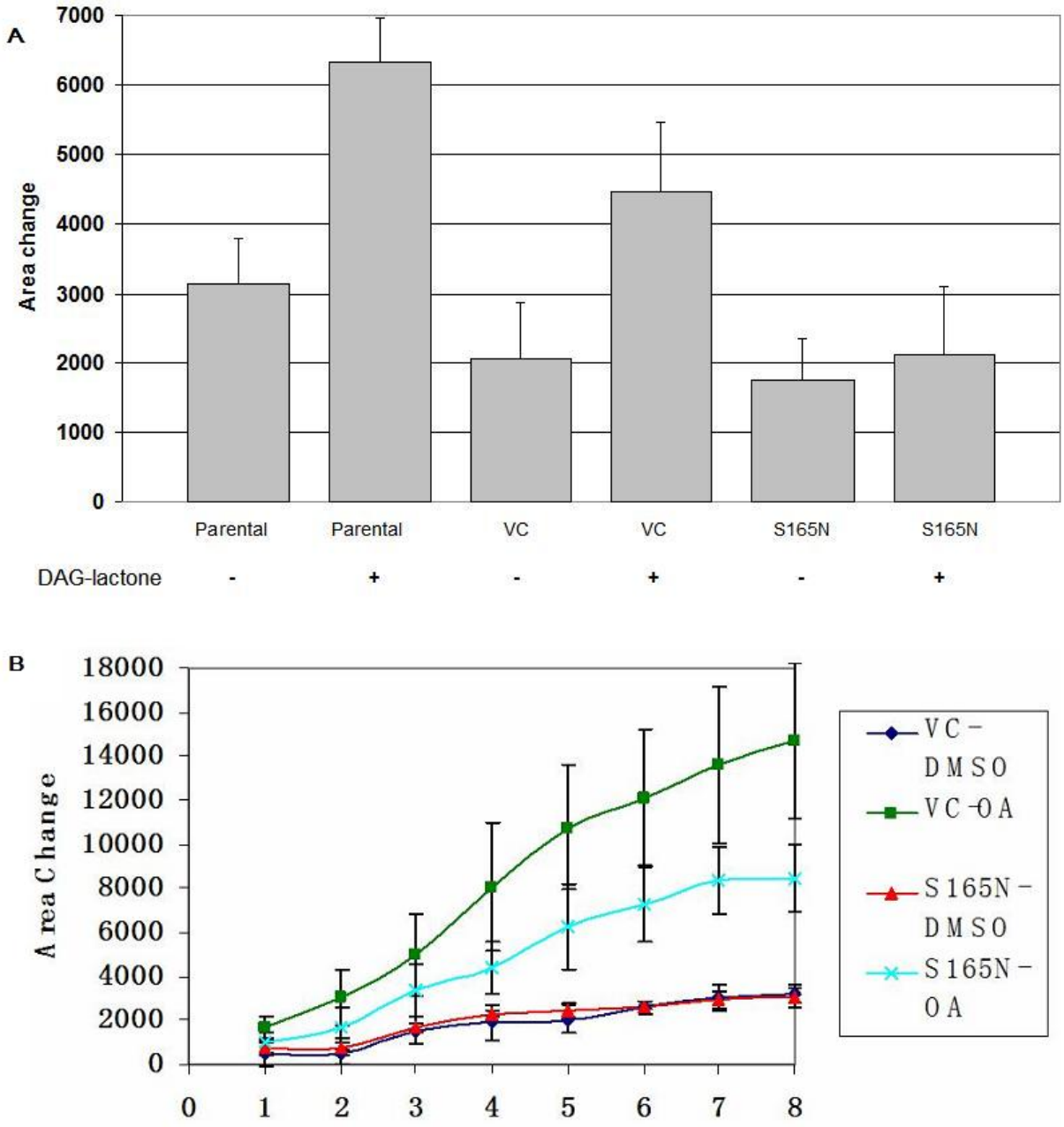

Figure 33. Motility of F1 cells transfected with phosphorylation-resistant mutants of α6-tubulin. (A) F1 cells were transfected with the phosphorylation-resistant mutant of α6-tubulin or the vector control (VC), followed by treatment with 5 μM DAG-lactone or DMSO (0.1% v/v) as vehicle control for the entire experimental period (6 h). (B) Motility of F1 cells was measured following transfection with S165N-α6-tubulin or the vector control (VC). Cells were treated with 1 μM OA or DMSO (0.1% v/v) for the entire experimental period (8 h). The extent of movement was analyzed at 1 h intervals for a total period of 8 h. All motility assays were carried out in triplicate, as described in 'Methods and Materials'.

established in B16 F1 mouse melanoma cells. Therefore, α6-tubulin mutants were examined in these cells for their effect on motile behavior. As shown in Figure 33A, DAG-lactone-stimulated B16 F1 cell motility was decreased to basal levels when cells were transfected with S165N-α6-tubulin. The same mutant also greatly reduced B16 F1 cell motility stimulated by OA in an analogous study (Figure 33B). Therefore, blockade of phosphorylation of S165 in α-tubulin interferes with the mechanism of motility induced by either DAG-lactone or OA.

Effect of S165N-α6-tubulin on cell motility produced by phospho-MARCKS.

Because MARCKS contributes two-thirds of the motility stimulated by OA, inhibition by S165N could be explained by its interference in phospho-MARCKS signaling. A possible relationship between α6-tubulin and MARCKS signaling in the motility pathway was investigated by co-expressing S165N-α6-tubulin and mutant GFP-MARCKS in B16 F1 cells. In Figure 34, motility assays showed that even though S165D-α6-tubulin alone could not increase motile behavior in these cells, S165N nonetheless produced a dominant-negative effect on motility engendered by pseudo-phosphorylated MARCKS mutant (DS-MARCKS).

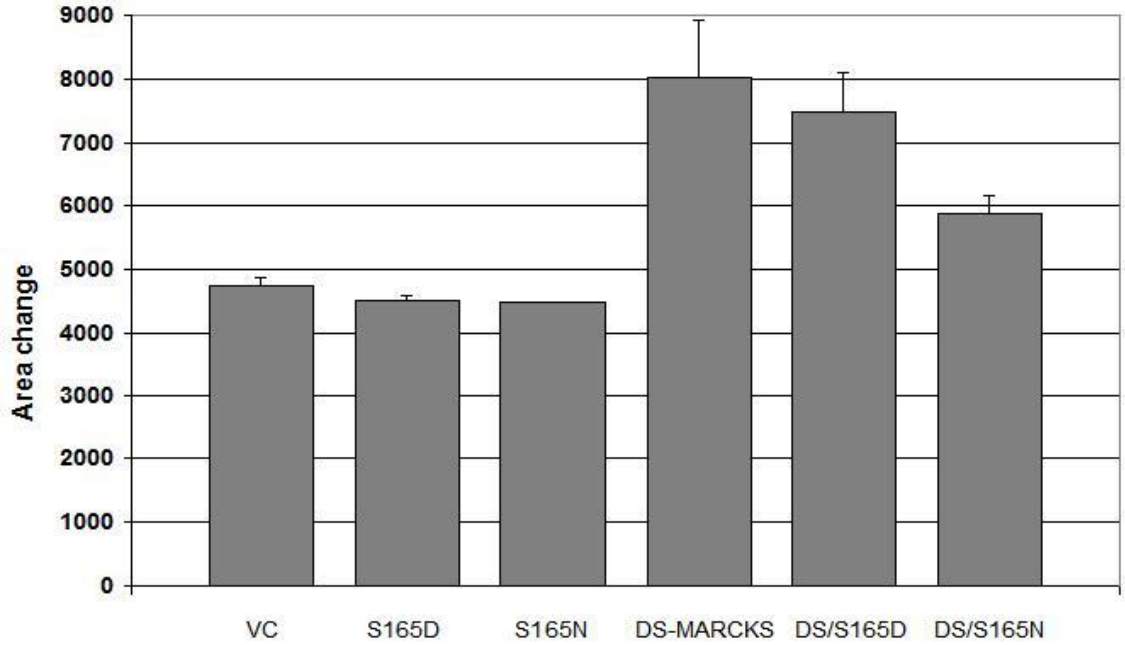

Figure 34. Effect on motility of F1 cells transfected with mutants of GFP-MARCKS and α6-tubulin. F1 cells were transfected with the pseudo-phosphorylated α6-tubulin mutant (S165D), the phosphorylation- resistant mutant (S165N) either alone or in combination with the pseudo-phosphorylated GFP-MARCKS (D/S), or the vector control (VC). Cell motility was measured after 6 h. All motility assays were carried out in triplicate, as described in 'Methods and Materials'.

MARCKS recycling in B16 F1 cells.

Previous studies with fibroblasts showed that MARCKS associated with the lysosomal compartment upon treatment with TPA. Upon removal of TPA, MARCKS returned to the membrane in a nocodazole-sensitive manner thereby implicating a role for microtubules in the recycling process (Allen and Aderem, 1995). This finding provided a possible linkage between MARCKS and microtubules. To investigate a possible interaction between MARCKS and microtubules, B16 F1 cells that had been transfected with GFP-WT-MARCKS were analyzed by confocal microscopy. As shown in Figure 35, GFP-WT-MARCKS translocated to the cytoplasm after treatment with DAG-lactone for 5 min followed by wash-out with PBS. Following removal of DAG-lactone, return of GFP-WT-MARCKS to the plasma membrane

was discernable within 2 h and was complete by 6h.

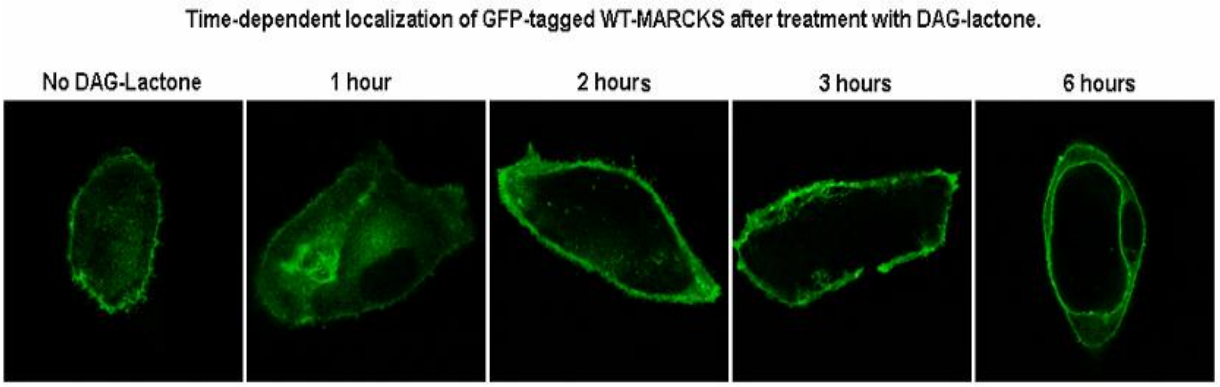

Figure 35. Time-dependent localization of GFP-tagged WT-MARCKS after brief treatment with DAG-lactone. F1 cells were transfected with GFP-WT-MARCKS followed by treatment with 5 μM DAG-lactone for 5 min. After 5 min, DAG-lactone was washed out with 1X PBS. The GFP signal was detected for a total time period of 6 h on a Leica vonfocal microscope and the images were representatives of the cells viewed.

Effect of S165N-α6-tubulin on MARCKS localization.

In view of the fact that PKCα phosphorylates α-tubulin, the question of whether this event is functionally inter-related with MARCKS recycling was addressed. To examine this potential relationship, the phosphorylation-resistant mutant of α6-tubulin (myc-tagged S165N) was expressed and an effect on the re-localization of GFP-WT-MARCKS was analyzed. For this experiment, B16 F1 cells were co-transfected with GFP-WT-MARCKS and myc-S165N-α6-tubulin. Confocal imaging (Figure 36) revealed that when S165N-α6-tubulin was overexpressed, GFP-WT-MARCKS remained in the cytoplasmic compartment after 6 h, presumably due to interrupted transport by microtubules.

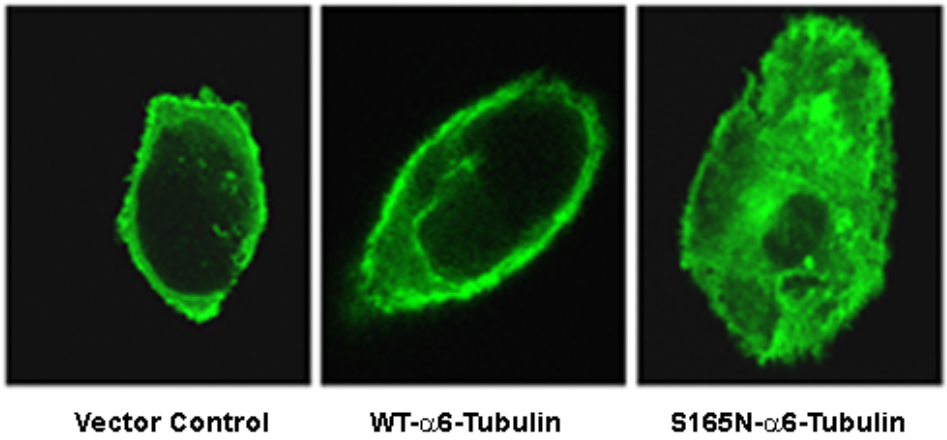

Figure 36. Effect of S165N-α6-tubulin on GFP-WT-MARCKS localization in B16 F1 cells. B16 F1 cells (cultured on a 6-well plate) were co-transfected with GFP-WT-MARCKS and WT-α6-tubulin, S165N-α6-tubulin or the vector control. Transfectants were treated for 5 min with 5 μM DAG-lactone followed by three washes with 1X PBS and the complete medium was restored. After 6 h, the medium was removed and the cells were fixed in 4% paraformaldehyde in 1X PBS. The GFP signal was detected on a Leica confocal microscope.

Since it was previously shown that the myc-tagged S165N mutant can be incorporated into microtubules (Figure 18), it was speculated that the mutation at Ser-165 (to Asn) prevented a direct interaction between WT-MARCKS and microtubules, thereby preventing the return of WT-MARCKS to the membrane. Because of the apparently high rate at which dephosphorylation of phosphoMARCKS occurs in F1 cells following DAG-lactone treatment (Figure 26A), the dephosphorylation reaction is not the limiting step. It could be that S165N-α6-tubulin inhibition of WT-MARCKS recycling is part of the mechanism by which this PKC-resistant mutant of α-tubulin inhibits motility (Abeyweera *et al.*, 2009).

Discussion

In the foregoing studies, MARCKS, a known substrate of PKC, was investigated for its role in the motility behavior of mouse melanoma cells that is part of the metastatic phenotype. As

described by a conventionally held model, MARCKS undergoes phosphorylation by PKC and consequently is released from the plasma membrane into the cytoplasm. This translocation enables actin rearrangements (Thelen *et al*., 1991; Blackshear, 1995). However, a cytoplasmic role for phospho-MARCKS had not been previously documented. In the present study, the findings support a model in which phospho-MARCKS promotes motility, primarily through protein-protein interactions through its phosphorylated effector domain.

These findings show that MARCKS is a major determinant in the motility phenotype of metastatic mouse melanoma cells. The observation that treatment with the phosphatase inhibitor okadaic acid led to both elevated phospho-MARCKS and increased B16 F1 cell motility, and that both decreased upon treatment with MARCKS shRNA, implies that there is highly active phosphatase activity operating in F1 cells to maintain a low metastatic potential. In this regard, initial experiments showed that over-expression of constitutively active PKCα stimulated B16 F1 cell motility to a modest degree but did not increase phospho-MARCKS (Figure 24). Similarly, DAG-lactone failed to induce phospho-MARCKS after 6 h treatment (Figure 25). One explanation is that DAG does not induce PKC to bind the plasma membrane with high affinity (Gopalakrishna and Barsky, 1988), and it is metabolized quickly in the cell. These observations support a model in which membrane PKC activity is high in B16 F1 cells but is being effectively countered by protein phosphatases. This model is also supported by studies with GFP-WT-MARCKS which was primarily localized to the membrane (Figure 29) and therefore was unphosphorylated. With OA treatment to inhibit phosphatases, GFP-WT-MARCKS accumulated in the cytoplasm, an event that was consistent with having

undergone phosphorylation by membrane-level PKC. It is concluded that the presence of highly active phosphatases, particularly PP1 and PP2A, provides a mechanism for the low metastatic behavior of B16 F1 cells.

A major finding of the present study is that phospho-MARCKS stimulates motility in the cytoplasmic compartment, as shown by the increased motility that results from expression of a cytoplasmic pseudo-phosphorylated MARCKS mutant (Figure 30). This function was further supported by a dominant-negative effect observed on OA-induced motility by a phosphorylation-resistant MARCKS mutant (A2G_N/S) that was also cytoplasmic due to the absence of the myristoyl group (Figure 28). This double mutant, whose cytoplasmic site of action was distinguished from that of the membrane-bound, myristoylated mutant (N/S-GFP-MARCKS), effectively blocked up to 50% of motility of OA-stimulated F1 cells and intrinsically motile F10 cells (Figure 32). Similar inhibitory effects on motility by this double mutant were observed with human cancer cell lines derived from various tissues, namely A375 melanoma cells (55% inhibition), MDA-MB-231 breast cells (55% inhibition), and LNCaP prostate cells (30% inhibition) (D. Fonseca, unpublished data), thereby suggesting widespread significance for cytoplasmic phospho-MARCKS function. In view of the dominant negative effect of the A2G_N/S double mutant, the presence of phosphate groups on MARCKS is likely to be a major structural determinant for productive interaction of MARCKS with its cytoplasmic target(s) and may therefore be independent of Ca^{2+}/calmodulin-dependent pathways. A recent study of human cholangiocarcinoma specimens and related cell lines reported a similar prominent role for cyoplasmic phosphoMARCKS in the invasion and

migration characteristics of biliary cancer (Techasen *et al.*, 2010). We speculate that phospho-MARCKS transmits the motility signal in the cytoplasm through its interactions with unknown binding proteins. Although a specific protein-protein interaction has yet to be defined, the identification of these binding partners could prove to be useful targets for future design of anti-metastasis drugs.

Preliminary experiments suggest that phosphorylation of Ser-165 in α-tubulin promotes an interaction between microtubules and MARCKS that consequently drives motile behavior. Alternatively, cytoplasmic phospho-MARCKS could be independent of microtubules while it propagates the motility signal and is only dependent on microtubules for recycling back to the membrane. These possibilities are depicted in the model given in Figure 37.

Our findings suggest interplay between two PKC substrates in a manner that drives cell movement. The model is supported by a previous finding by the laboratory of A. Aderem that MARCKS recycles to the plasma membrane via microtubules (Allen and Aderem, 1995), thus defining a structural interaction between MARCKS and microtubules. The present work (Figure 36) demonstrated that S165N-α6-tubulin expression in F1 cells led to an interruption in the return of GFP-WT-MARCKS to the membrane following transient treatment with DAG-lactone. This finding suggests that phosphorylation of S165 in α6-tubulin by PKC promotes the recycling process of MARCKS that is being mediated by microtubules. Additional findings demonstrated that the S165N mutant of α6-tubulin also interfered with motility of OA-treated F1 cells (Figure 33), as well as F1 cell motility induced by

over-expression of the pseudophosphorylated MARCKS mutant (Figure 34). While these preliminary results imply that there is potential for interplay between two proteins phosphorylated by PKC, future studies are required to explore the nature of this interaction.

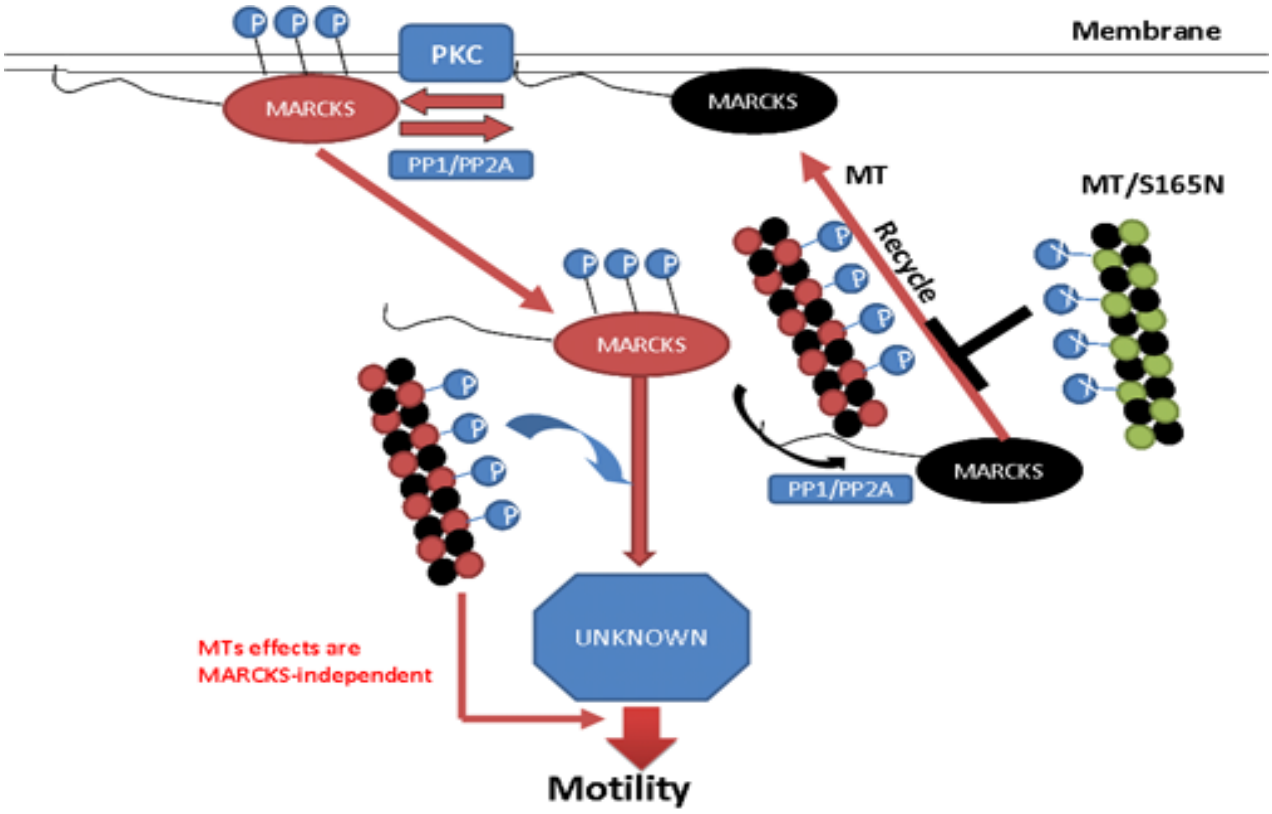

Figure 37. Model of MARCKS and microtubules in the motility pathway.

If microtubules have a mechanistic role in promoting phospho-MARCKS signaling, it is speculated that phospho-MARCKS requires phospho-α-tubulin in microtubules to access its binding partners at specific intracellular locations. Therefore, interruption of MARCKS recycling by the mutation at Ser-165 may have represented only the return segment of a more extensive transport process whereby phospho-MARCKS that is borne as cargo by microtubules, gains access to specific binding partners. Our pilot studies have not shown any evidence of MARCKS co-localization with either microtubules (using anti-α-tubulin) or lysosomes (using

anti-LAMP) (data not shown). Another candidate site is the microtubule organizing center (MTOC) that was previously identified as a MARCKS binding site (Michaut *et al*., 2005). In this regard, the newly identified PKC substrate CEP4 could also participate in the MARCKS-driven motility pathway given that it is a downstream effector of Cdc42, which is believed to be involved in directed cell movement through MicroTubule Organizing Centers (MTOCs) that are oriented towards the leading edge (Nobes and Hall, 1995). Whether there is a possible linkage between phospho-MARCKS and CEP4 through MTOCs deserves further investigation.

Future studies will explore the trafficking of MARCKS to specific locations and to identify any protein binding partners, including CEP4 as a possible candidate. Several experiments are proposed as follows: (1) Test the effect of nocodazole in DS-MARCKS transfected or okadaic acid treated cells to establish the role of intact microtubules in phospho-MARCKS stimulated motility; (2) Co-stain phospho-MARCKS and cellular compartments such as Golgi apparatus and other organelles to determine DAG-lactone-induced localization of this phospho-protein in melanoma cells; (3) Immunoprecipitate phospho-MARCKS in okadaic acid-treated cells in detergent-free buffer to identify any potential binding partners when compared to control cells treated with DMSO. CEP4 could be probed in the pellet to test whether it is a binding partner of MARCKS; (4) If potential phospho-MARCKS binding partners were revealed from (3), a mutational analysis could be performed for these binding proteins and the mutants tested subsequently to assess their effect on cell motility.

Concluding Statement

The work described here demonstrated the successful identification of potential PKC substrates using the Traceable Kinase Method and characterized the role of PKC substrates in the motile behavior of cancer cells. This approach revealed several potential PKC substrates including known PKC substrates (Table 2). Among the identified potential substrates, cdc42-EP4 (CEP4) has been verified as an in-vitro PKCα and δ substrate. As an example of these potential substrates shown to have a physiological role, a novel PKCα substrate α6-tubulin, was identified by the Rotenberg laboratory using the Traceable Kinase Method (Abeyweera and Rotenberg, 2007). α6-Tubulin was found to participate in the motility pathway triggered by a known PKC substrate, MARCKS, whose phosphorylation promotes a previously undocumented cytoplasmic role in motile behavior. A phosphorylation-resistant mutant of α6-tubulin (S165N-α6-tubulin) was shown to inhibit cell motility engendered by over-expression of a pseudophosphorylated MARCKS mutant (DS-MARCKS) in mouse melanoma cells. Interestingly, the same α6-tubulin mutant blocked the recycling of MARCKS to the membrane. It is concluded that PKC-mediated phosphorylation of these two PKC substrates and their potential interplay contribute to cell motility, thereby providing an avenue for future study.

REFERENCES

Abeyweera T.P. Use of the traceable kinase method to identify protein substrates that mediate PKCα-stimulated motility in human breast cells. Ph.D. Dissertation, The Graduate Center of The City University of New York, 2007.

Abeyweera T.P., Chen X. and Rotenberg S.A. Phosphorylation of α6-tubulin by protein kinase Cα activates motility of human breast cells. *J. Biol. Chem*. 284: 17648-17656, 2009

Abeyweera T.P. and Rotenberg S.A. Design and characterization of a traceable protein kinase C-alpha. *Biochemistry* 46: 2364-2370, 2007

Alberts B., Johnson A., Lewis J., Raff M., Roberts K., and Walter P. Molecular Biology of the Cell. (4th edition), p. 1325, Garland Publishing, 2002

Allen L.A. and Aderem A. Protein kinase C regulates MARCKS cycling between the plasma membrane and lysosomes in fibroblasts. *EMBO J.* 14: 1109-1121, 1995

Alt A., Gartzbein M., Ohba M., Kuroki T., and Tennenbaum T. Differential regulation of alpha6beta4 integrin by PKC isoforms in murine keratinocytes. *Biochem. Biophys. Res. Commun*. 314: 17-23, 2004

Arbuzova A., Schmitz A.A.P., and Vergeres G. Cross-talk unfolded: MARCKS proteins. *Biochem. J.* 362: 1-12, 2002

Ballestrem C., Wehrle-Haller B., Hinz B., and Imhof B. A. Actin-dependent lamellipodia formation and microtubule-dependent tail retraction control-directed cell migration. *Mol. Biol. Cell*, 11: 2999-3012, 2000

Becker D., Beebe S.J., and Herlyn M. Differential expression of protein kinase C and cAMP-dependent protein kinase in normal human melanocytes and malignant melanomas. *Oncogene* 5: 1133-1139, 1990

Blackshear P.J. The MARCKS family of cellular protein kinase C substrates. *J. Biol. Chem.* 268: 1501-1504, 1995

Bourbon N.A., Yun J., and Kester M. Ceramide directly activates protein kinase C ζ to regulate a stress-activated protein kinase signaling complex. *J. Biol. Chem.* 275: 35617-35623, 2000

Bryan J., and Kane R.E. Separation and interaction of the major components of sea urchin actin gel. *J. Mol. Biol.* 125: 207-224, 1978

Caloca M.J., Fernandez M.N., Lewin N.E., Ching D., Modali R., Blumberg P.M. and Kazanietz M.G. β2-chimaerin is a high affinity receptor for the phorbol ester tumor promoters.

J. Biol. Chem. 272: 26488-26494, 1997

Castagna M., Takai Y., Kaibuchi K., Sano K., Kikkawa U. and Nishizuka Y. Direct activation of calcium-activated, phospholipid-dependent protein kinase by tumor-promoting phorbol esters. *J. Biol. Chem*. 257: 7847-51, 1982

Chen X. and Rotenberg S.A. Phospho-MARCKS drives motility of mouse melanoma cells. *Cell. Signal.* 22: 1097-1103, 2010

Chitaley, K., Chen, L, Galler, A., Walter, U., Daum, G., and Clowes, A.W. (2004) Vasodilator-stimulated phosphoprotein is a substrate for protein kinase C. *FEBS Lett*. **556**: 211-215.

Clarke P.R., Siddhanti S.R., Cohen P., and Blackshear P.J. Okadaic acid-sensitive phosphatases dephosphorylated MARCKS, a major protein kinase C substrate. *FEBS Lett*. 336: 37-42, 1993

Dempsey E.C., Newton A.C., Mochly-Rosen D., Fields A.P., Reyland M.E., Insel P.A., and Messing R.O. Protein kinase C isozymes and the regulation of diverse cell responses. *Am. J. Physiol.* 279: L429-L438, 2000

Disatnik M.H., Boutet S.C., Pacio W., Chan A.Y., Ross L.B., Lee C.H. and Thomas R.A. The bi-directional translocation of MARCKS between membrane and cytosol regulates integrin-mediated muscle cell spreading. *J. Cell Sci.* 117: 4469-4479, 2004

Ekker L.V., and Parker P.J. Protein kinase C-a question of specificity. *Trends Biochem. Sci.* 19: 73-77, 1994

Estrada-Bernal A., Gatlin J.C., Sunpaweravong S., and Pfenninger K. Dynamic adhesions and MARCKS in melanoma cells. *J. Cell Sci.* 122: 2300-2310, 2009

Fidler I.J. Selection of successive tumour lines for metastasis. *Nature New Biol*. 242: 148-149, 1973

Flynn D.C., Leu T.H., Reynolds A.B., and Parsons J. T. Identification and sequence analysis of cDNAs encoding a 110-kilodalton actin filament-associated pp60src substrate. *Mol. Cell. Biol.* 13: 7892-7900, 1993

Friedl, P. and Brocker, E.-B. T cell migration in three-dimensional extracellular matrix: guidance by polarity and sensations. *Dev. Immunol*. 7: 249-266, 2000

Galvez A.S., Duran A., Linares J.F., Panthrose P., Castilla E.A., Abu-Baker S., Loitges M., Diaz-Meco M.T. and Moscat J. Protein kinase C zeta represses the interleukin-6 promoter and impairs tumorigenesis in vivo. *Mol. Cell Biol.* 1: 104-115, 2009

Garcia-Bermejo M.L., Leskow F.C., Fuji T., Wang Q., Blumberg P.M., Ohba M., Kurok T., Han K.C., Lee J., Marquez V.E., and Kazanietz M.G.. Diacylglycerol (DAG)-lactones, a new class of protein kinase C (PKC) agonists, induce apoptosis in LNCaP prostate cancer cells by selective activation of PKCalpha. *J. Biol. Chem.* 277: 645-655, 2002

Gardner K. and Bennett V. A new erythrocyte membrane-associated protein with calmodulin binding activity. *J. Biol. Chem*. 261: 1339-1348, 1986

Gauthier, M.L., Torretto, C., Ly, J., Francescutti, V., and O'Day, D.H. Protein kinase Calpha negatively regulates cell spreading and motility in MDA-MB-231 human breast cancer cells downstream of epidermal growth factor receptor. *Biochem. Biophys. Res. Commun.* 307: 839-846, 2003

Ghoul A., Serova M., Benhadji K. A., Cvitkovic E., Faivre S., Philips E., Calvo F., Lokiec F., and Raymond E. Protein kinase C α and δ are members of a large kinase family of high potential for novel anticancer targeted therapy. *Targ. Oncol.* 1: 42-53, 2006

Gopalakrishna R., and Barsky S.H. Tumor promoter-induced membrane-bound protein kinase C regulates hematogenous metastasis. *Proc. Natl. Acad. Sci.* 85: 612-616, 1988

Gordon P.R., and Gilchrest B.A. Human melanogenesis is stimulated by diacylglycerol. *J. Invest. Dermatol.* 93: 700-702, 1989

Graff J.M., Stumpo D.J., and Blackshear P.J. Characterization of the phosphorylation sites in the chicken and bovine myristoylated alanine-rich C kinase substrate protein, a prominent cellular substrate for protein kinase C. *J. Biol. Chem.* 264: 11912-11919, 1989

Grohmanova K., Schlaepfer D., Hess D., Gutierrez P., Beck M., and Kroschewski R. Phosphorylation of IQGAP1 modulates its binding to Cdc42, revealing a new type of rho-GTPase regulator. *J. Biol. Chem.* 279: 48495-48504, 2004.

Iwabu A., Smith K., Allen F.D., Lauffenburger D.A., and Wells A. Epidermal growth factor induces fibroblast contractility and motility via a protein kinase Cδ-dependent pathway. *J. Biol. Chem*. 279: 14551-14560, 2004

Kennelly P.J. and Krebs E.G.. Consensus sequences as substrate specificity determinants for protein kinases and protein phosphatases. *J. Biol. Chem.* 266**:** 15555-15558, 1991

Kerfoot C., Huang W., and Rotenberg, S.A. Immunohistochemical analysis of advanced human breast carcinomas reveals down-regulation of protein kinase Cα. *J. Histochem. Cytochem.* 52: 419-422, 2004

Kikkawa U., Kishimoto A., and Nishizuka Y. The protein kinase C family: heterogeneity and its implications. *Ann. Rev. Biochem.* 58: 31-44, 1989

Kiley S.C., Clark K.J., Duddy S.K., Welch D.R., and Jaken S. Increased protein kinase Cδ in mammary tumor cells: relationship to transformation and metastatic progression. *Oncogene* 18: 6748-6757, 1999

Koivunen J., Aaltonen V., and Peltonen J. Protein kinase C (PKC) family in cancer progression. *Cancer Lett.* 235: 1-10, 2005

Kureishy N, Sapountzi V, Prag S, Anilkumar N., and Adams J.C. Fascins and their roles in cell structure and function. *Bioessays* 24: 350-361, 2002

Ladwein M., and Rottner K. On the Rho'd: The regulation of membrane protrusions by Rho-GTPases. *FEBS Lett*. 582: 2066–2074, 2008

Larsson C. Protein kinase C and the regulation of the actin cytoskeleton. *Cell. Signal.* 18: 276-284, 2006

Ling E., Gardner K., and Bennett V. Protein kinase C phosphorylates a recently identified membrane skeleton-associated calmodulin-binding protein in human erythrocytes. *J. Biol. Chem*. 261: 13875-13878, 1986

Liu B., Renaud C., Nelson K.K., Chen Y.Q., Bazaz R., Kowynia J., Timar J., Diglio C.A., and Honn K.V. Protein kinase C inhibitor calphostin C reduces B16 amelanotic melanoma cell adhesion to endothelium and lung colonization. *Int. J. Cancer* 52: 147-52, 1992

Liu Y., Shah K., Yang F., Witucki L., and Shokat K.M. Engineering src family protein kinases with unnatural nucleotide specificity. *Chem. Biol.* 5: 91-101, 1998

Mao, M., Fang, X., Lu, Y., Lapushin, R., Bast, R.C., and Mills, G..B. Inhibition of growth-factor-induced phosphorylation and activation of protein kinase B/Akt by atypical protein kinase C in breast cancer cells. *Biochem. J.* 352: 475-482, 2000

McKiernan E., O'Brien K., Grebenchtchikov N., Geurts-Moespot A., Sieuwerts A.M., Martens J.W.M., Magdolen V., Evoy D., McDermott E., Crown J., Sweep F.C.G.J., and Duffy M.J. Protein kinase Cδ expression in breast cancer cells as measured by real-time PCR, western blotting and ELISA. *Brit. J. Cancer* 99: 1644-1650, 2008

Meisinger J., Patel S., Vellody K., Bergstrom R., Benefield J., Lozanoa Y. and Young M. Protein phosphatase-2A association with microtubules and its role in restricting the invasiveness of human head and neck squamous cell carcinoma cells. *Cancer Lett.* 111: 87-95, 1997

Mellor H. and Parker P.J. The extended protein kinase C superfamily. *Biochem. J.* 332: 281-292, 1998

Michaut M.A., Williams C.J. and Schultz R.M. Phosphorylated MARCKS: A novel centrosome component that also defines a peripheral subdomain of the cortical actin cap in mouse eggs. *Developmental Biology* 280: 26-37, 2005

Morrison, E.E., B.N. Wardleworth, J.M. Askham, A.F. Markham, and D.M. Meredith. EB1, a protein which interacts with the APC tumour suppressor, is associated with the microtubule cytoskeleton throughout the cell cycle. *Oncogene* 17: 3471–3477, 1998

Murray A.W., Dournier A.F., and Hardy S.J. Proteolytic activation of protein kinase C: a physiological reaction? *Trends Biochem. Sci*. 12: 53-54, 1987

Newton A.C. Regulation of the ABC kinases by phosphorylation: protein kinase C as a paradigm. *Biochem. J.* 370: 361-371, 2003

Nishizuka Y. The role of protein kinase C in cell surface signal transduction and tumor promotion. *Nature* 308: 693-698, 1984

Nishizuka Y. The family of protein kinase C for signal transduction. *JAMA* 262:1826-1833, 1989

Ng T., Shima D., Squire A., Bastiaens P.I.H., Gschmeissner S., Humphries M.J., and Parker P.J. PKC-α regulates β1 integrin-dependent cell motility through association and control of integrin traffic. *EMBO J.* 18: 3909-3923, 1999

Nobes C.D., and Hall A. Rho, rac, and cdc42 GTPases regulate the assembly of multimolecular focal complexes associated with actin stress fibers, lamellipodia, and filopodia. *Cell* 81: 53-62, 1995

Oka M., and Kikkawa U. Protein kinase C in melanoma. *Cancer and Metastasis Rev.* 24: 287-300, 2005

Osmanagic-Myers S., and Wiche G.. Plectin-RACK1 (receptor for activated C kinase 1) scaffolding: a novel mechanism to regulate protein kinase C activity. *J. Biol. Chem*. 279:18701-18710, 2004

Pietromonaco S.F., Simons P.C., Altman A., and Elias L. Protein kinase C-θ phosphorylation of moesin in the actin-binding sequence. *J. Biol. Chem*. 273: 7954-7603, 1998

Qian Y., Baisden J.M., Cherezova L., Summy J.M., Guappone-Koay A., Shi X.L., Mast T., Henry J.P., Zot G., Mazloum N., Lee M.Y., and Flynn D.C. PKC phosphorylation increases the ability of AFAP-110 to cross-link actin filaments. *Mol. Biol. Cell*. 13: 2311-2322, 2002

Rabinowitz I., Tsomo L., and Mercurio A.M. PKCα phosphorylation of specific serines in the connecting segment of the β4 integrin regulates the dynamics of type II hemidesmosomes. *Mol.*

Cell Biol. 24: 4351-4360, 2004

Rombouts K., Lottini B., Caligiuri A., Liotta F., Mello T., Carloni V., Marra F., and Pinzani M. MARCKS is a downstream effector in platelet-derived growth factor-induced cell motility in activated human hepatic stellate cells. *Exp. Cell Res.*314: 1444-1454, 2008

Sanz-Navarez E., Fernandez N., Kazanietz M.G. and Rotenberg S.A. Atypical protein kinase C zeta suppresses migration of mouse melanoma cells. *Cell Growth Differ.* 10: 517-24, 2001

Shah K., Liu Y., Deirmengian C. and Shokat K.M. Engineering unnatural nucleotide specificity for Rous sarcoma virus tyrosine kinase to uniquely label its direct substrates. *Proc. Natl. Acad. Sci. U.S.A.* 94: 3565-3570, 1997

Shah K. and Shokat K.M. A chemical genetic screen for direct v-src substrates reveals ordered assembly of a retrograde signaling pathway. *Chem. Biol.* 9: 35-47, 2002

Spizz G. and Blackshear P.J. Overexpression of the myristoylated alanine-rich C-kinase substrate inhibits cell adhesion to extracellular matrix components. *J Biol. Chem.* 276: 32264-32273, 2001

Sukai M., and Mochly-Rosen D. Pharmacologic modulation of protein kinase C isozymes: the role of RACKs and subcellular localization. *Pharmacol. Res.* 39: 253-259, 1999

Sullivan R.M., Stone M., Marshall J.F., Uberall F., and Rotenberg S.A. Photo-induced inactivation of protein kinase Cα by dequalinium inhibits motility of murine melanoma cells. *Mol. Pharmacol.* 58: 729-737, 2000

Sun, X.-g., and Rotenberg, S.A., Overexpression of protein kinase Cα in MCF-10A human breast cells engenders dramatic alterations in morphology, proliferation, and motility. *Cell Growth Diff.* 10: 343-352, 1999

Techasen A., Loilome W., Namwat N., Takahashi E., Sugihara E., Puapairoj A., Miwa M., Saya H., and Yongvanit P. Myristoylated alanine-rich C kinase substrate phosphorylation promotes cholangiocarcinoma cell migration and metastasis via the protein kinase C-dependent pathway. *Cancer Sci.* 101:658-665, 2010.

Thelen M., Rosen A., Nairn A.C., and Aderem A. Regulation by phosphorylation of reversible association of a myristoylated protein kinase C substrate with the plasma membrane. *Nature* 351: 320-322, 1991

Ting A.Y., Witte K., Shah K., Kraybill B., Shokat K.M., and Schultz P.G. Phage-display evolution of tyrosine kinases with altered nucleotide specificity. *Biopolymers* 60: 220-228, 2001

Ueda Y., Syu-ichi H., and Osada S. Protein kinase C-δ activates the MEK-ERK pathway in a manner independent of Ras and dependent on Raf. *J. Biol. Chem.* 271: 23512-23519, 1996

Urtreger A.J., Grossoni V.C., Falbo K.B., Kazanietz M.G., and Joffe E. Atypical protein kinase C-ζ modulates clonogenicity, motility, and secretion of proteolytic enzymes in murine mammary cells. *Mol. Carcinogenesis*, 42: 29-39, 2005

Vaughan K.T. TIP maker and TIP marker: EB1 as a master controller of microtubule plus ends. *J. Cell Biol.* 171: 197–200, 2005

Wetsel W.C., Khan W.A. and Merchenthaler I. Tissue and cellular distribution of the extended family of protein kinase C isoenzymes. *J. Cell. Biol.* 117: 121-133, 1992

Werth D.K. and Pastan I. Vinculin phosphorylation in response to calcium and phorbol esters in intact cells. *J. Biol. Chem*. 259: 5264-5270, 1983

Witucki L.A., Huang X., Shah K., Liu Y., Hyin S., Eck M.J. and Shokat K.M. Mutant tyrosine kinases with unnatural nucleotide specificity retain the structure and phospho-acceptor specificity of the wildtype enzyme. *Chem. Biol.* 9: 25-33, 2002

Wu W.C., Walaas S.I., Nairn A.C., Greengard P., and Blackshear P.J. Calcium/phospholipid regulates phosphorylation of a M_r "87kD" substrate protein in brain synaptosomes. *Proc. Natl. Acad. Sci. U.S.A.* 79: 5249-5253, 1982

Zheng J.H., Knighton D.R., ten Eyck L.F., Karlsson R., Xuong N.H., Taylor S.S., and Sowadski J.M. Crystal structure of the catalytic subunit of cAMP-dependent protein kinase complexed with magnesium-ATP and peptide inhibitor. *Biochemistry* 32: 2154-2161, 1993